

Phthalocyanine-Based Organic Thin-Film Transistors: A Review of Recent Advances

Owen A. Melville,[†] Benoît H. Lessard,^{*,†,∇} and Timothy P. Bender^{*,†,‡,§}

[†]Department of Chemical Engineering and Applied Chemistry, University of Toronto, 200 College Street, Toronto, Ontario, Canada M5S 3E5

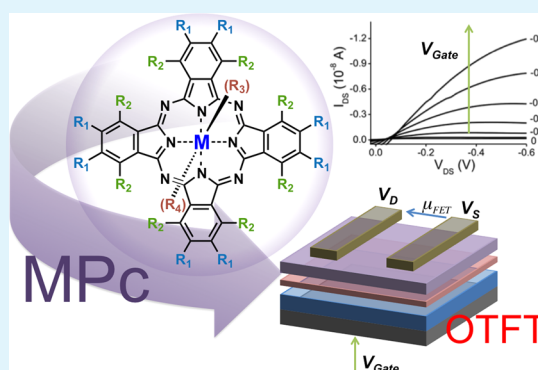
[‡]Department of Materials Science and Engineering, University of Toronto, 184 College Street, Toronto, Ontario, Canada M5S 3E4

[§]Department of Chemistry, University of Toronto, 80 St. George Street, Toronto, Ontario, Canada M5S 3H6

[∇]Department of Chemical and Biological Engineering, University of Ottawa, 161 Louis Pasteur, Ottawa, Ontario, Canada, K1N 6N5

ABSTRACT: Metal phthalocyanines (MPcs) are versatile conjugated macrocycles that have attracted a great deal of interest as active components in modern organic electronic devices. In particular, the charge transport properties of MPcs, their chemical stability, and their synthetic versatility make them ideal candidate materials for use in organic thin-film transistors (OTFTs). This article reviews recent progress in both the material design and device engineering of MPc-based OTFTs, including the introduction of solubilizing groups on the MPcs and the surface modification of substrates to induce favorable MPc self-assembly. Finally, a discussion on emerging niche applications based on MPc OTFTs will be explored, in addition to a perspective and outlook on these promising materials in OTFTs. The scope of this review is focused primarily on the advances made in the field of MPc-based OTFTs since 2008.

KEYWORDS: phthalocyanine, organic, electronic, thin, film, field-effect, transistor



INTRODUCTION

Organic thin film transistors (OTFTs) are an integral part of numerous flexible electronic applications such as smart cards, electronic paper, radio frequency identification (RFID) tags, sensors, electronic postage, and labels, as well as the circuitry for flexible matrices of organic light-emitting diodes (OLEDs).^{1–3} The use of organic materials has several advantages such as relatively low processing temperatures, potential compatibility with plastic substrates, and broad chemical tunability for ease of modification and device enhancement.

The OTFT is based on a three-electrode design, where the source and drain electrodes are directly in contact with a layer of semiconducting organic molecules and the third gate electrode is electrically insulated by a dielectric. When a small gate voltage (V_G) is applied, little current flows across the organic semiconductor between the source and the drain when applying a bias (V_{ds}) between them. Therefore, this device is considered “off”. As the V_G becomes greater than a threshold voltage (V_T), the current flow (I_d) between the source and drain is facilitated and the device is considered “on”. OTFTs are evaluated on the basis of their ability to effectively switch states, in particular with a low magnitude V_T , a high on-to-off current ratio (I_{ON}/I_{OFF}), and a high field-effect mobility (μ).⁴ Over the years, various organic small molecules and polymer materials, along with numerous different OTFT device

configurations, have been explored, and their application has been discussed in great detail in several reviews.^{1–3,5–9} The two most common OTFT structures are the bottom-gate, top-contact (BGTC) and the bottom-gate, bottom-contact (BGBC) configurations (Figure 1). The descriptions of the configuration refer to the placement of the electrodes relative to the semiconductive organic layer and are visually represented in Figure 1.

Phthalocyanines (Pcs) are composed of a nitrogen-linked tetrameric diiminoisoindoline conjugated macrocycle (Figure 2). Pcs can often chelate a metal or metalloid through two covalent bonds and two coordination bonds resulting in a highly stable material (MPc) that can be used for a variety of applications including dyes and pigments, and as active materials in organic electronic devices.^{8,10–15} The precursors for the synthesis of most MPcs are relatively inexpensive and can be obtained from major chemical manufacturers in large quantities. This consideration makes MPcs favorable for numerous commercial applications and is why numerous industrial laboratories are still exploring their use in a variety of applications. Since the early 1970s, Xerox Corporation has developed a patent position on the use of metal-free Pc and

Received: February 24, 2015

Accepted: May 22, 2015

Published: May 22, 2015

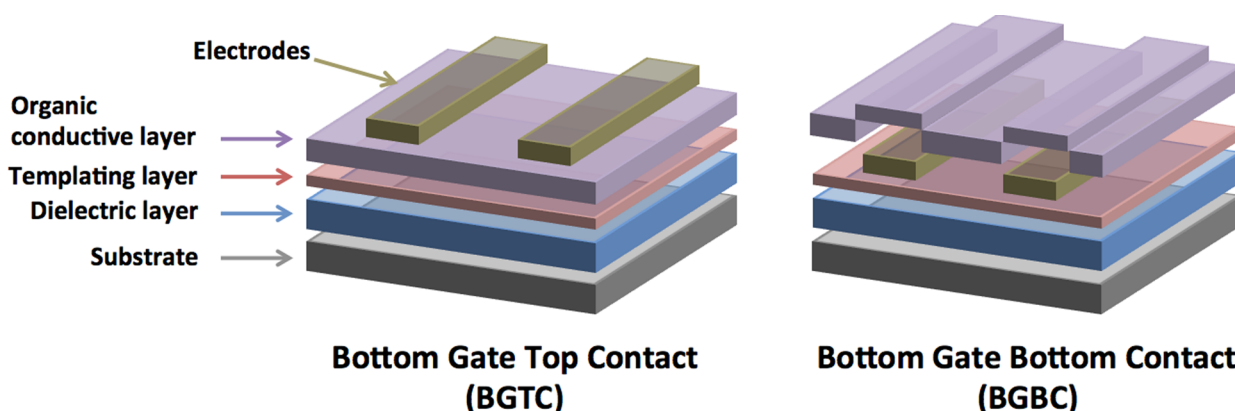


Figure 1. Top-contact (left) and bottom-contact (right) configuration for organic thin film transistors. In both cases, the gold electrodes denote the source/drain and the gate is on the bottom (gray substrate).

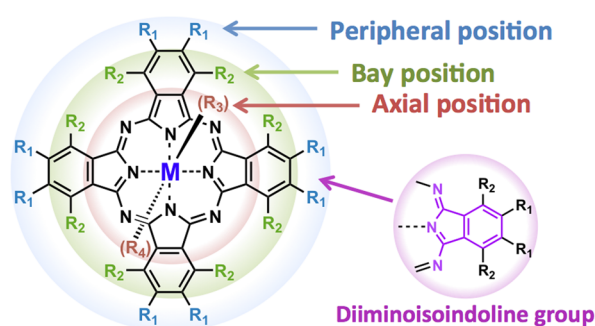


Figure 2. Metal phthalocyanine (MPc) molecular structure with descriptive terminologies for relevant positions around the molecule highlighted.

several MPcs such as copper Pc (CuPc), gallium Pc, titanium Pc, silicon Pc, germanium Pc, tin Pc, and others for use as inks, dyes, and pigments, as well as for use as the active material in both photovoltaic devices and xerographic organic photo-receptors.^{16–24} Several other companies have also patented the use of MPcs as inks and electrophotographic materials such as Canon, Inc.,²⁵ Lexmark International, Inc.,¹⁹ and Avicia Limited.²⁶ To this day, functionalized CuPcs are still considered one of the most common pigments used in cyan toners and inks.^{22,24}

Depending on the application, it is common to functionalize the MPc either by directly modifying it or by performing its synthesis with a functionalized phthalonitrile and corresponding metal halide. Over 95 different elements have been successfully incorporated into Pcs.²⁷ Common functionalizations take place in the axial position (central atom), the peripheral or/and the bay positions of the MPcs (Figure 2). These added molecular fragments can change the solubility, solid-state arrangement, or even photophysical properties of the corresponding material.^{8,13–15}

Over the years, a great deal of interest has been directed toward including these materials in organic electronic devices, because of their high charge transport properties, strong absorbance, and ease of synthesis. The molecular planarity of MPcs, as well as their ability to stack and their tendency to form crystalline and polycrystalline films make them ideal candidates for OTFTs. Table 1 is a tabulation of some of the most current and best performing nonfunctionalized/unmodified MPc-based OTFTs organized by metal inclusion. Corresponding charge carrier mobilities are also tabulated. In addition to the different metal inclusion, several other parameters are identified, such as the device structure, the inducing layer, and the processing conditions.

This review article outlines recent advances for MPc-based OTFTs. The review is bucketed into several sections, outlining the use of soluble MPcs, the variation of processing conditions,

Table 1. Best Reported Field-Effect Performances for Unmodified Phthalocyanines in OTFTs by Metal

MPc	gate/insulator	inducing layer (thickness)	source-drain (SD) contact	structure	deposit temp (°C)	μ [type] ($\text{cm}^2 \text{V}^{-1} \text{s}^{-1}$)	ref
TiOPc	Si/SiO ₂	OTS	Au	BGTC	110	1–10 [P]	28
VOPc	Si/SiO ₂	F2-P4T (6 nm)	Au	BGTC	170	2.6 [P]	29
SnOPc	Si/SiO ₂	<i>p</i> -6p (9 nm)	Au	BGTC	180	0.44 [N]	30
ZnPc	Si/SiO ₂	<i>p</i> -6p (2 nm)	Au	BGTC	180	0.32 [P]	31
CuPc	Si/SiO ₂	<i>p</i> -6p	Au	BGTC	180	0.18 [P]	32
F ₁₆ CuPc	Si/SiO ₂	<i>p</i> -6p (2 nm)	Au	BGTC	180	0.11 [N]	31
MgPc	SiO ₂ /parylene-C	none	Au	BGTC	not reported	0.021 [P]	33
PbPc	Pt/Ionic liquid	none	Pt	TGBC	480	0.01 [P]	34
H ₂ Pc	Si/SiO ₂	none	Au	BGBC	125	2.6×10^{-3} [P]	35
FePc	Si/SiO ₂	none	Au	BGBC	125	6.9×10^{-4} [P]	35
PdPc	Si/SiO ₂	none	Au	BGTC	~25	6.2×10^{-4} [P]	36
NiPc	Si/SiO ₂	none	Au	BGBC	200	5.4×10^{-4} [P]	35
PtPc	Si/SiO ₂	none	Au	BGBC	125	1.5×10^{-4} [P]	35
SnPc	Si/SiO ₂	none	Au	BGBC	30	7.3×10^{-5} [P]	35
BsubPc	Au/parylene-C	none	CaAg	BGTC	not reported	5.4×10^{-5} [N]	37

Table 2. Best Reported Field-Effect Performances for Solution-Processed Phthalocyanines by Metal

base MPC	μ ($\text{cm}^2 \text{V}^{-1} \text{s}^{-1}$)	substituent (number)	inducing layer	device structure	annealing conditions		ref
					temp ($^{\circ}\text{C}$)	time (min)	
Eu ₂ Pc ₃	1.7	–octanaphthoxy (16)	HMDS	BGTC	100	30	42
NiPc	1.1	–SO ₃ Na (1.5)	none	BGBC	50	20	41
TiOPc	0.92	–C ₈ H ₁₇ (4)	OTS	BGTC	100		39
CuPc	0.70	–C ₆ H ₁₃ (4)	ODTS	BGBC	100	30	40
VOPc	0.40	–C ₈ H ₁₇ (4)	OTS	BGTC	120		39
CoPc	0.20	–SO ₃ Na (1.5)	none	BGBC	50	20	41
ZnPc	0.02	–SO ₃ Na (1.5)	none	BGBC	50	20	41
AlPc ₂	0.02	–SO ₃ Na (1.5)	none	BGBC	50	20	41
LuPc ₂	8×10^{-3}	–C ₈ H ₁₇ (16)	OTS	BGTC	70		43

the addition or modification of various OTFT components (inducing layer, insulating layer, SD contacts), and their use in niche applications. The scope of this review is focused primarily on the advances made to the field of MPC-based OTFTs since the 2008 review by Li et al.⁸

SOLUTION-PROCESSED PHTHALOCYANINES

Most metal phthalocyanines (MPCs) are not inherently soluble and therefore are processed by vacuum vapor deposition to fabricate organic thin film transistors (OTFTs). Although there are some exceptions, such as sodium phthalocyanine,³⁸ most MPCs need to have solubilizing groups (such as alkyl chains) attached to their periphery in order to be amenable for the use of solution processing techniques such as spin-coating or inkjet printing. Fortunately, a good deal of progress has been made in improving the performance of OTFTs made from solution-processed MPCs since 2007, when the highest field-effect mobility (μ) achieved was $1.7 \times 10^{-3} \text{ cm}^2 \text{V}^{-1} \text{s}^{-1}$.⁸ Table 2 summarizes the best performing devices using solution-processed MPCs that have been reported to date. The best devices of this type now boast μ approaching^{39,40} or even exceeding⁴¹ $1 \text{ cm}^2 \text{V}^{-1} \text{s}^{-1}$. The following paragraphs summarize the individual efforts that have led to developments in this area.

It has been shown that the arrangement of solubilizing groups attached to the periphery of the MPC can affect the solid-state packing and, thus, charge-transport properties in the film. Wang et al. were able to produce OTFTs with μ values as high as $0.96 \text{ cm}^2 \text{V}^{-1} \text{s}^{-1}$, using the titanium oxide MPC (TiOPc) analogue (**1**, Figure 3), and $0.4 \text{ cm}^2 \text{V}^{-1} \text{s}^{-1}$ for the corresponding vanadium oxide MPC (VOPc) analogue (**2**, Figure 3).³⁹ The authors claimed, based on XRD data, that the

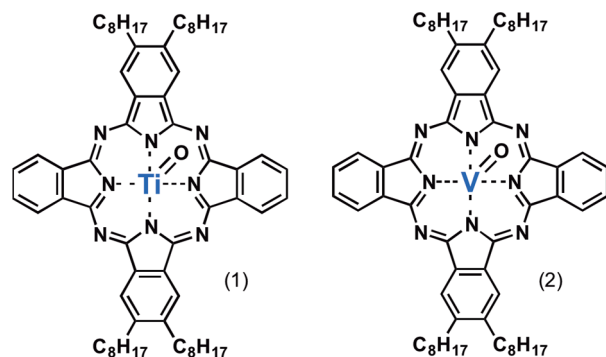


Figure 3. Solution-processable titanium and vanadium phthalocyanines with peripheral alkyl attachments used in thin-film transistors.

placement of the alkyl groups forced them to intercolate between phthalocyanine layers without interfering with π -stacking along the other planar direction. The authors further proposed that this gives the molecules the ability to self-assemble at room temperature, with thermal annealing increasing the μ of TiOPc devices by only 4% and VOPc devices by 25%. The length of the alkyl attachments was also a factor. For both the VOPc and TiOPc derivative, the ideal number of carbons in the chains was 8, although good performance was also observed for 12 and 6 carbons. Overall, these devices showed excellent performance, with high on-to-off current ratio, $I_{\text{ON}}/I_{\text{OFF}} = 10^5$ – 10^6 and relatively low threshold voltages ($V_T = 4.4 \text{ V}$ to -15 V).

Another important factor in device performance is isomerism. The tetraoctyl-substituted VOPc (**3**) has 4 isomers (**4**–**7**), when their attachment is limited to the bay sites on the outlying rings (Figure 4). When the isomers were not separated, the result was a lower liquid crystal transition temperature, and their incorporation into top contact OTFTs yielded devices with μ values as high as $0.017 \text{ cm}^2 \text{V}^{-1} \text{s}^{-1}$ ⁴⁴ and $0.012 \text{ cm}^2 \text{V}^{-1} \text{s}^{-1}$ ⁴⁵. In comparison, purified isomers such as (**5**) performed worse, with a maximum μ value of $4.5 \times 10^{-4} \text{ cm}^2 \text{V}^{-1} \text{s}^{-1}$, or better, such as isomer **6**, with a maximum μ value of $0.13 \text{ cm}^2/(\text{V s})$.⁴⁵ The better performing isomers (**4** and **6**), in this case, had lower π – π stacking distances, as determined by XRD, and had a tendency to form larger grains when annealed. At first glance, steric repulsion between alkyl groups could serve as an explanation; however, in that case, **4** should outperform **6**, which it does not. Thus, the film-forming properties of various isomers of solution-processed MPCs may be difficult to predict.

The modified zinc MPC (ZnPc) (**8**) has four oxygen-containing groups attached to the periphery of the phthalocyanine without specific isomerism (Figure 5). Basic devices without an inducing layer or an annealing step during fabrication produced μ as high as $4.4 \times 10^{-6} \text{ cm}^2 \text{V}^{-1} \text{s}^{-1}$.⁴⁶ Since compound **8** was shown to be liquid crystalline at a low temperature, annealing at a relatively low temperature of $70 \text{ }^{\circ}\text{C}$ was shown to increase μ to $1.0 \times 10^{-4} \text{ cm}^2 \text{V}^{-1} \text{s}^{-1}$, with an $I_{\text{ON}}/I_{\text{OFF}}$ of 10^4 and a V_T of 3 V .⁴⁷ A further increase in μ to $1.8 \times 10^{-4} \text{ cm}^2 \text{V}^{-1} \text{s}^{-1}$ is observed when a silicon dioxide insulating layer is modified with an octyltrichlorosilane (OTS, **13**) monolayer⁴⁸ (see Figure 6).

Eight identical substituent groups can be grafted to the bay sites of the outlying fused rings of a MPC. Such a MPC is symmetric and does not have the same structural isomers as mentioned in the preceding paragraph MPCs. OTFTs fabricated using octadecyltrichlorosilane (ODTS, **14**, Figure 6) as a templating monolayer and completely bay-position alkyl-functionalized copper MPCs (CuPcs, **9**; see Figure 5) as the

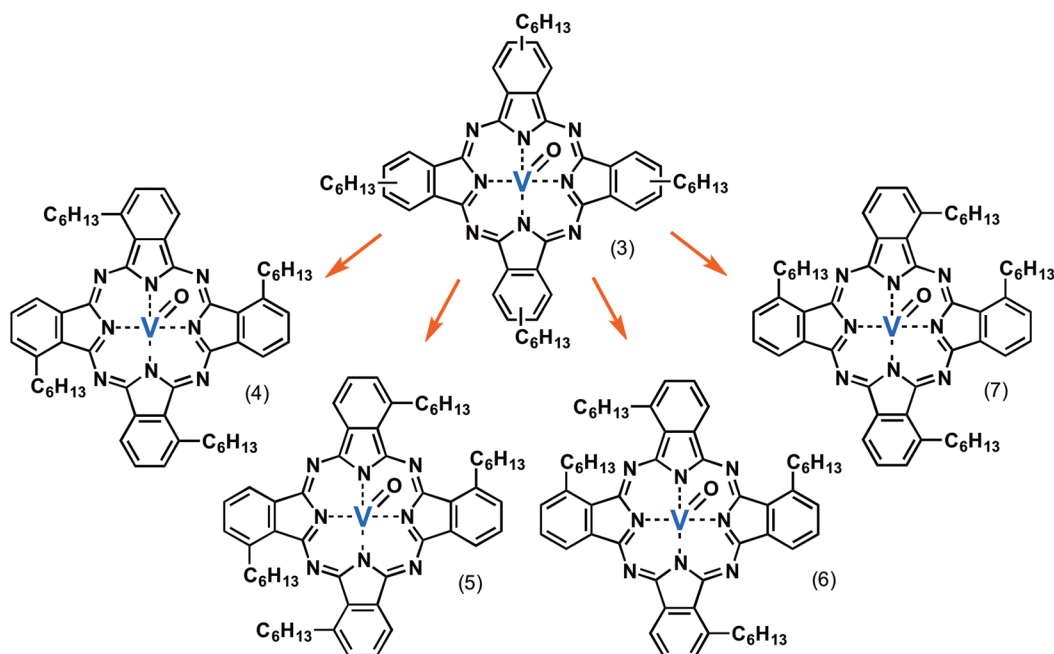


Figure 4. Four isomers of a solution-processable vanadium phthalocyanine with four alkyl chains substitutions in the bay positions.

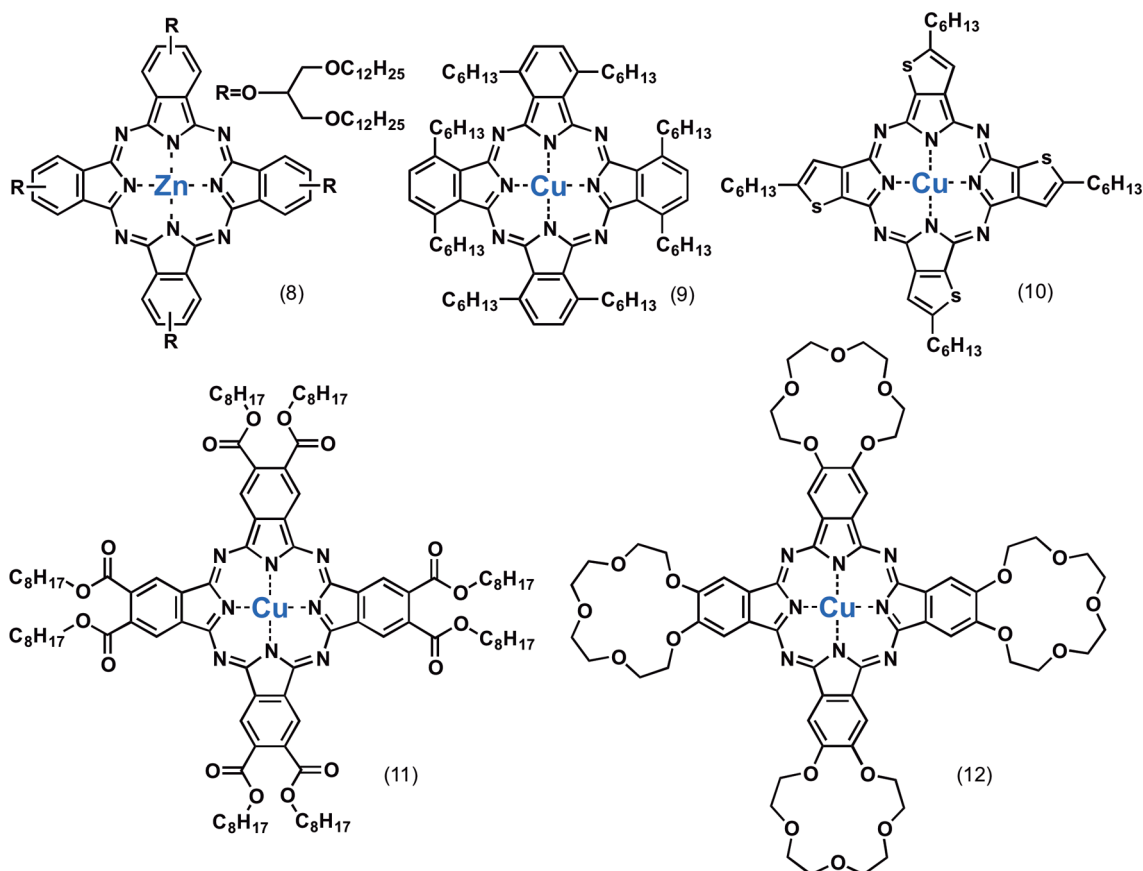


Figure 5. Various solution-processed phthalocyanines used in thin-film transistors.

active layer were characterized as having μ values as high as $0.02 \text{ cm}^2 \text{ V}^{-1} \text{ s}^{-1}$ without annealing⁴⁹ and $0.70 \text{ cm}^2 \text{ V}^{-1} \text{ s}^{-1}$ with annealing.⁴⁰ The high μ value was partly attributed to the edge-on orientation of the CuPc molecules in the thin film and the relatively large average grain size of 62 nm.⁴⁰ This is the highest μ reported for a solution-processed CuPc derivative in an

OTFT, and the high $I_{\text{ON}}/I_{\text{OFF}} = 10^7$ and low $V_T = -1 \text{ V}$ for the optimized devices makes this MPC a good candidate for integration into more-complex electronics.

Lutetium bisphthalocyanine (LuPc₂) was also modified in a similar fashion with a hexyl group on each of its phthalocyanine rings. According to a reported study, this compound is

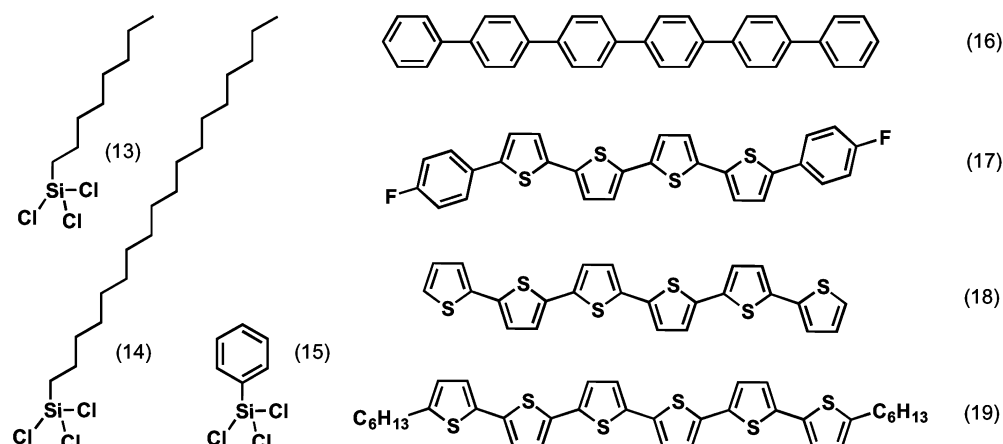


Figure 6. Small molecules used for the inducing layers of phthalocyanine OTFTs: octyltrichlorosilane (OTS, 13) and octadecyltrichlorosilane (ODTS, 14), phenyltrichlorosilane (PTS, 15), *para*-sexiphenylene (*p*-6p, 16), fluorobenzene-capped thiophene oligomer (F2-P4T, 17), α -sexithiophene (α 6T, 18), and α,α' -dihexylsexithiophene (DH- α 6T, 19).

thermotropic liquid crystalline and undergoes a phase transition at 62 °C and, thus, can only be annealed at 70 °C.⁴³ Bottom-contact transistors produced with an OTS templating layer demonstrated a μ value as high as $8 \times 10^{-3} \text{ cm}^2 \text{ V}^{-1} \text{ s}^{-1}$, with $I_{\text{ON}}/I_{\text{OFF}} = 10^5$ and $V_T \approx -13 \text{ V}$.

Phthalocyanines can be arranged into other complex structures, such as stacks or dimers. OTFTs produced using solution-processable zinc and cobalt MPCs (2',10',16',24'-(6,6'-methylenebis[2(2-hydroxy)-5-methylbenzyl]-4-methyl)-bis-(oxidiphthalocyaninato-dizinc(II)) and 2',10',16',24'-(6,6'-methylenebis[2(2-hydroxy)-5-methylbenzyl]-4-methyl)-bis-(oxidiphthalocyaninato-dicobalt(II))) had a hole μ value (μ_{hole}) of $2.8 \times 10^{-3} \text{ cm}^2 \text{ V}^{-1} \text{ s}^{-1}$ and $7.3 \times 10^{-3} \text{ cm}^2 \text{ V}^{-1} \text{ s}^{-1}$, respectively, after thermal annealing.⁵⁰

Recently, Chen and co-workers investigated the use of a series of bis(phthalocyaninato) (EuPc_2)- and tris(phthalocyaninato) (Eu_2Pc_3)-based complexes in solution-processed BGTC OTFTs. The group functionalized the peripheral positions of all or some of the MPCs with phenoxy⁵¹ and naphthoxy^{42,52} groups. The resulting sandwich complexes were introduced into OTFTs by the solution-based quasi-Langmuir–Shäfer (QLS) method⁵³ reporting ambipolar (both *p*- and *n*-channel) mobilities. Interestingly, OTFTs made from the phenoxy functional Eu_2Pc_3 ⁵¹ were ambipolar and characterized by having $\mu_{\text{elect}} = 0.68 \text{ cm}^2 \text{ V}^{-1} \text{ s}^{-1}$ and $\mu_{\text{hole}} = 0.014 \text{ cm}^2 \text{ V}^{-1} \text{ s}^{-1}$, while those made from the naphthoxy functional EuPc_2 ⁵² were found to have $\mu_{\text{hole}} = 0.10 \text{ cm}^2 \text{ V}^{-1} \text{ s}^{-1}$ and $\mu_{\text{elect}} = 0.01 \text{ cm}^2 \text{ V}^{-1} \text{ s}^{-1}$, respectively. The same authors also found that the performance of OTFTs made using naphthoxy functional Eu_2Pc_3 s could be significantly improved by employing a solvent annealing step in dichlorobenzene at 100 °C for 30 min, resulting in high and balanced carrier mobilities of $\mu_{\text{hole}} = 1.7 \text{ cm}^2 \text{ V}^{-1} \text{ s}^{-1}$ and $\mu_{\text{elect}} = 1.3 \text{ cm}^2 \text{ V}^{-1} \text{ s}^{-1}$.⁴² The group has also explored the use of phenoxy functional bis(phthalocyaninato)(porphyrinato) europium complexes obtaining similar ambipolar OTFTs with $\mu_{\text{elect}} = 0.30 \text{ cm}^2 \text{ V}^{-1} \text{ s}^{-1}$ and $\mu_{\text{hole}} = 0.16 \text{ cm}^2 \text{ V}^{-1} \text{ s}^{-1}$ when using a thin layer of CuPc as an inducing layer.⁵⁴ Typical I_d vs V_G and I_d vs V_{ds} plots for this MPC compound can be found in Figure 7 without the CuPc-inducing layer (Figure 7A) and with the inducing layer (Figure 7B).

So far, most OTFTs discussed in this section have been *p*-type. Indeed, few examples of *n*-type solution-processed MPC in

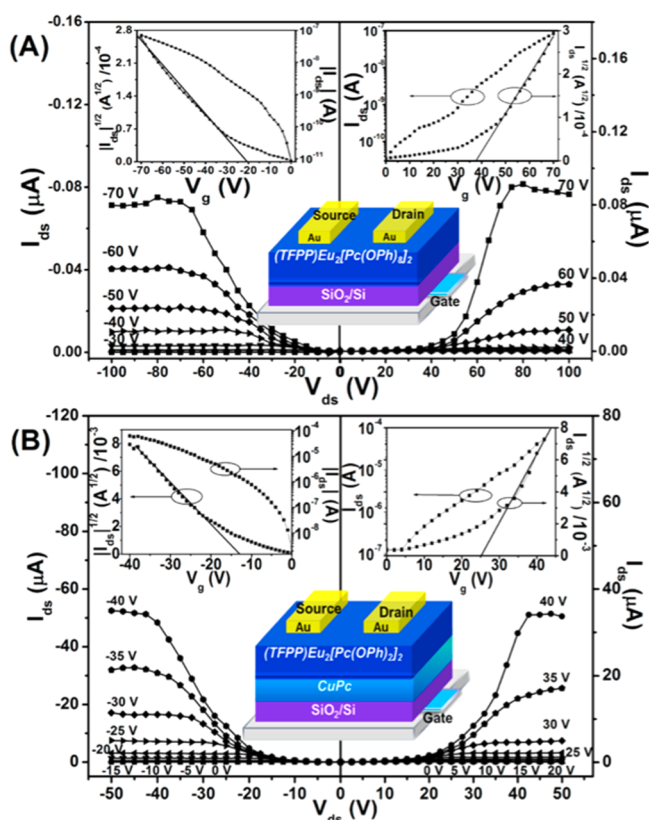


Figure 7. Output characteristics (I_{ds} vs V_{ds}) and (insets) transfer characteristics ($I_{ds}^{1/2}$ vs V_G), as well as device configurations of ambipolar OTFTs based on (A) the single-component (TFPP)Eu₂[Pc(OPh)₈]Eu[Pc(OPh)₈] QLS film and (B) the two-component (TFPP)Eu₂[Pc(OPh)₈]Eu[Pc(OPh)₈]/CuPc heterojunction deposited on SiO₂/Si substrate with Au top contact measured in air. (Reprinted with permission from Dameng et al.⁵⁴ Copyright 2015, American Chemical Society.)

OTFTs exist in the literature. The most common strategy for creating an *n*-type MPC is to attach electron-withdrawing fluorines in all 16 peripheral and bay positions; the prototypical example is F₁₆CuPc.⁵⁵ While F₁₆CuPc is insoluble, one method to bestow solubility is to attach solubilizing groups, such as those with alkyl attachments. In one study, octyloxycarbonyl substituents (also electron-withdrawing) were attached to CuPc

to produce **10** and OTFTs were fabricated with this as the active layer and hexadimethylsilane (HDMS) as the inducing layer and μ_{elect} values as high as $1.6 \times 10^{-4} \text{ cm}^2 \text{ V}^{-1} \text{ s}^{-1}$ were achieved (see Figure 5).⁵⁵ In the same study, the authors varied the peripheral substituents, replacing some or all of the octyloxy carbonyl groups with electron-donating crown ether groups. Except in the case of **11** (Figure 5), all of these compounds functioned in *n*-type OTFTs, but with inferior μ values than the aforementioned example. Devices using **11** were *p*-type, demonstrating a relatively high μ_{hole} of $0.06 \text{ cm}^2 \text{ V}^{-1} \text{ s}^{-1}$.

One interesting example of a solution-processable MPC relative used in an OTFT is the tetra-(5-hexylthiophene)-fused copper macrocycle (**10**, Figure 5). Although an exact CuPc analogue does not exist in the literature, OTFTs manufactured using this active layer and an inducing layer of OTS had a maximum μ of $0.2 \text{ cm}^2 \text{ V}^{-1} \text{ s}^{-1}$,⁵⁶ superior to that of the similarly substituted vanadyl⁴⁵ ($0.13 \text{ cm}^2 \text{ V}^{-1} \text{ s}^{-1}$) and zinc⁴⁶ ($1.8 \times 10^{-4} \text{ cm}^2 \text{ V}^{-1} \text{ s}^{-1}$) phthalocyanines as used in OTFTs.

While most reports have focused on attaching alkyl groups to bestow solubility upon the phthalocyanines, there are certainly other possibilities. Sodium salts of various sulfonated MPCs, including nickel, copper, cobalt, zinc, and aluminum, are soluble and were utilized in bottom-gate OTFTs with no inducing layer.⁴¹ These devices showed generally high μ_{hole} , with a device composed of a mixture of monosulfonated and disulfonated nickel MPC (NiPc) demonstrating a μ value of $1.1 \text{ cm}^2 \text{ V}^{-1} \text{ s}^{-1}$, which, at that time, was a record value for solution-processed phthalocyanine derivatives. Despite having such a high μ value, such devices had relatively low $I_{\text{ON}}/I_{\text{OFF}}$ ratios of 10^3 , because of the innately high conductivity and ionic nature of the films. Certainly, further study utilizing an inducing layer or high-dielectric insulating layer might produce even higher-performing OTFTs.

■ THE EFFECT OF A TEMPLATING/INDUCING LAYER ON MPC OTFT PERFORMANCE

Many OTFTs utilize a thin layer between the insulating dielectric layer and the active layer, sometimes called the inducing layer, interlayer, or templating layer. This layer can improve the performance of OTFTs by reducing the concentration of electron or hole traps in the active layer⁵⁷ and by providing a template for the growth of the MPC layer.^{29,58–60} It is well-known that the orientation and the degree of π - π stacking between semiconducting molecules plays a significant role in the OTFT performance,^{61–63} and, therefore, the choice of inducing layer is critical. Some of the materials used for inducing layers to achieve these effects in MPC OTFT devices are illustrated in Figure 6.

Kim et al. studied the changes in morphology and device performance for CuPc transistors on both ODTs-modified (hydrophobic) and $\text{H}_2\text{SO}_4/\text{H}_2\text{O}_2$ -modified (hydrophilic) silicon wafers.⁶⁴ After depositing CuPc at room temperature onto the modified surfaces, they found that the grains on the hydrophobic surface were more randomly distributed in size and orientation but were more densely packed. The authors suggest this density difference, maintained after thermal annealing up to $180 \text{ }^\circ\text{C}$, was responsible for the order of magnitude difference ($10^{-3} \text{ cm}^2 \text{ V}^{-1} \text{ s}^{-1}$, compared to $10^{-4} \text{ cm}^2 \text{ V}^{-1} \text{ s}^{-1}$) between the μ values of CuPc devices deposited on the hydrophobic and hydrophilic surfaces, respectively.

Both octyltrichlorosilane (OTS, **13**, Figure 6) and octadecyltrichlorosilane (ODTS, **14**, Figure 6) are commonly used to treat SiO_2 surfaces in MPC-based OTFTs. This process does

not require vacuum deposition of an additional layer and can be done by relatively simple surface chemistry/treatment on the Si/ SiO_2 substrates. In one study, the μ value for CuPc OTFTs improved from $1.5 \times 10^{-3} \text{ cm}^2 \text{ V}^{-1} \text{ s}^{-1}$ for the bare substrate to $3.8 \times 10^{-3} \text{ cm}^2 \text{ V}^{-1} \text{ s}^{-1}$ for the substrate treated with ODTs, and the authors attributed this difference to the reduction of traps at the interface between SiO_2 and CuPc.⁶⁵ A solution-processed CuPc derivative in a bottom-contact OTFT showed an increase from $2 \times 10^{-3} \text{ cm}^2 \text{ V}^{-1} \text{ s}^{-1}$ to $4 \times 10^{-2} \text{ cm}^2 \text{ V}^{-1} \text{ s}^{-1}$ with a similar treatment, with the authors calculating a decrease in trap density both at the CuPc/ SiO_2 interface and at the grain boundaries in the CuPc.⁴⁹ OTS has also been used for the fabrication of TiOPc-based OTFTs, resulting in the greatest reported μ value ($\sim 10 \text{ cm}^2 \text{ V}^{-1} \text{ s}^{-1}$) of all reported MPC-based OTFT devices. This extremely high μ value was attributed to the favorable π -stacking of the TiOPc molecules.²⁸

Depositing a hydrophobic inducing layer can reduce the interaction between the disordered insulating surface (typically SiO_2) and the MPC active layer.³¹ The slow formation of a thin film by vacuum deposition on such an inducing layer is called weak epitaxial growth (WEG) and has been used to produce some of the best-performing MPC-based OTFTs.^{29,31,32} One molecule that can be used in this way is *para*-sexiphenylene, *p*-6p (**16**, Figure 6). Tin oxide MPC (SnOPc) OTFTs with a *p*-6p inducing layer deposited at $180 \text{ }^\circ\text{C}$ achieved a maximum μ_{elect} value of $0.44 \text{ cm}^2 \text{ V}^{-1} \text{ s}^{-1}$ with a 9 nm *p*-6p layer.³⁰ In the same study, OTFTs produced on bare SiO_2 and with an OTS inducing layer produced maximum $\mu_{\text{elect}} = 1 \times 10^{-3} \text{ cm}^2 \text{ V}^{-1} \text{ s}^{-1}$ and $0.07 \text{ cm}^2 \text{ V}^{-1} \text{ s}^{-1}$, respectively. AFM imagery of the films showed that the largest grain sizes were for SnOPc deposited on *p*-6p, followed by OTS and then the bare substrate.

A similar study of the effect of *p*-6p thickness on film growth and OTFT performance was performed using CuPc.³² The authors found that grains of CuPc grown on *p*-6p deposited at $180 \text{ }^\circ\text{C}$ were more ordered and preferentially oriented as the thickness of *p*-6p increased to 2.4 monolayer equivalents (ML). OTFTs produced on these films demonstrated a maximum μ value of $0.18 \text{ cm}^2 \text{ V}^{-1} \text{ s}^{-1}$ at this same thickness and decreased thereafter. Since the V_T increases above 0.8 ML, the authors suggest that the *p*-6p layer actually increases the number of hole traps, but improves the quality of the film enough to increase the value of μ . A similar tradeoff between μ and another desirable property, $I_{\text{ON}}/I_{\text{OFF}}$, can be observed for SnOPc.³⁰ Despite this issue, $0.18 \text{ cm}^2 \text{ V}^{-1} \text{ s}^{-1}$ is the highest μ value yet achieved for nonmodified, polycrystalline CuPc OTFTs. ZnPc and F_{16}CuPc OTFTs that use a *p*-6p inducing layer have also achieved record μ values of $0.32 \text{ cm}^2 \text{ V}^{-1} \text{ s}^{-1}$ and $0.11 \text{ cm}^2 \text{ V}^{-1} \text{ s}^{-1}$, respectively.³¹

Para-sexiphenylene is not the most effective inducing layer for all MPCs. For VOPc, the incorporation of a fluorobenzene-capped thiophene oligomer (F2-P4T, **17**, Figure 6) into a OTFT as the inducing layer resulted in an air-stable transistor with a maximum μ value of $2.6 \text{ cm}^2 \text{ V}^{-1} \text{ s}^{-1}$, which is a record for all MPC-based transistors.²⁹ AFM characterization of the films suggested a large grain size with high interconnectivity between grains, while XRD testing found that the direction of π -stacking of the VOPc molecules was parallel to the substrate, as is generally desirable. In addition to a strong μ value, these OTFTs also had excellent $I_{\text{ON}}/I_{\text{OFF}}$ ratios between 10^6 and 10^7 and a V_T value between -1 V and -5 V . The authors suggest that the F atoms in the oligomer layer might increase the built-in electric field and decrease the value of V_T . For comparison, VOPc OTFTs with a *p*-6p inducing layer had a maximum μ

value of $1.5 \text{ cm}^2 \text{ V}^{-1} \text{ s}^{-1}$, with a V_T value between -9 V and -15 V and an $I_{\text{ON}}/I_{\text{OFF}}$ of 10^6 .

Other thiophene oligomers that are used in the literature for inducing layers include α -sexithiophene ($\alpha 6\text{T}$, **18**, Figure 6) and α,α' -dihexylsexithiophene (DH- $\alpha 6\text{T}$, **19**, Figure 6). Baba et al. found that the value of μ increased by a factor of ~ 100 , to $0.245 \text{ cm}^2 \text{ V}^{-1} \text{ s}^{-1}$ in TiOPc OTFTs, using a submonolayer of DH- $\alpha 6\text{T}$ above the SiO_2 gate dielectric.⁶⁶ XRD analysis of the TiOPc films found that they were well-ordered, with an edge-on orientation and π -stacking parallel to the substrate that is favorable to high μ values in OTFTs. Another study found that CuPc OTFTs using a 6 nm $\alpha 6\text{T}$ layer and a 4 nm DH- $\alpha 6\text{T}$ layer had the highest μ value of $0.11 \text{ cm}^2 \text{ V}^{-1} \text{ s}^{-1}$ and $0.085 \text{ cm}^2 \text{ V}^{-1} \text{ s}^{-1}$, respectively, compared to transistors with different inducing layer thicknesses and a control device with a μ value of $0.021 \text{ cm}^2 \text{ V}^{-1} \text{ s}^{-1}$.⁶⁷ AFM imagery of CuPc deposited on the optimal inducing layers revealed the films had larger grains and fewer gaps than CuPc films deposited on inducing layers with other thicknesses. The V_T value for the $\alpha 6\text{T}$ device was -7 V , compared to -13 V for the DH- $\alpha 6\text{T}$ device. Therefore, on all accounts, $\alpha 6\text{T}$ is the better inducing layer material for CuPc, whereas DH- $\alpha 6\text{T}$ is better for TiOPc. Variations in optimal inducing layer thickness and type should be expected, given the variation in MPC shape and properties (for instance, TiOPc is nonplanar⁶⁶).

Thin layers of polymers can also be used to modify the dielectric gate insulator and change the electronic properties of the active layer. For the solution-processable VOPc derivative (**3**, Figure 4) (where the alkyl chain is an octyl group), the highest field-effect μ ($0.017 \text{ cm}^2 \text{ V}^{-1} \text{ s}^{-1}$) was for a device with a 100 nm polyimide layer above the SiO_2 insulator, compared with ODTs ($2.5 \times 10^{-3} \text{ cm}^2 \text{ V}^{-1} \text{ s}^{-1}$) and phenyltrichlorosilane (PTS, **15**, $6.8 \times 10^{-3} \text{ cm}^2 \text{ V}^{-1} \text{ s}^{-1}$).⁴⁴ OTFTs with VOPc deposited on a 3 nm layer (on SiO_2) demonstrated ambipolar charge transport with a $\mu_{\text{elect}} = 7.8 \times 10^{-3} \text{ cm}^2 \text{ V}^{-1} \text{ s}^{-1}$ and a $\mu_{\text{hole}} = 1.3 \times 10^{-2} \text{ cm}^2 \text{ V}^{-1} \text{ s}^{-1}$.⁶⁸ In the same study, a 3 nm poly(vinyl alcohol) (PVA) inducing layer produced an n -type OTFT, with an $\mu_{\text{elect}} = 2.9 \times 10^{-3} \text{ cm}^2 \text{ V}^{-1} \text{ s}^{-1}$. The authors used XRD to confirm that the VOPc formed different phases on the different polymers, demonstrating that the inducing layer can not only affect the quality of film, but also its phase and the type of charge transport.

Another compound that can be used as an inducing layer is tetratetracontane (TTC), a straight-chain alkane containing 44 C atoms. One study compared top-contact CuPc OTFTs using either 20 nm TTC or poly(methyl methacrylate) (PMMA) as inducing/templating layers on a SiO_2 dielectric.⁶⁹ Using AFM imaging, they found that, while PMMA formed itself a smoother surface than TTC, the CuPc deposited on TTC formed larger, more ordered grains than on PMMA. Transport in both OTFTs was found to be ambipolar, with the TTC-based devices demonstrating both superior $\mu_{\text{elect}} = 5.8 \times 10^{-3} \text{ cm}^2 \text{ V}^{-1} \text{ s}^{-1}$ and $\mu_{\text{hole}} = 1.9 \times 10^{-2} \text{ cm}^2 \text{ V}^{-1} \text{ s}^{-1}$, compared to PMMA-based OTFTs with $\mu_{\text{elect}} = 2.7 \times 10^{-4} \text{ cm}^2 \text{ V}^{-1} \text{ s}^{-1}$ and $\mu_{\text{hole}} = 1.9 \times 10^{-3} \text{ cm}^2 \text{ V}^{-1} \text{ s}^{-1}$. Another study found that annealing the TTC layer at $60 \text{ }^\circ\text{C}$ for 2 h improved its regularity and the performance of CuPc devices deposited on it.⁵⁰ The minimum TTC thickness required for optimal device operation was $\sim 18 \text{ nm}$, after which the devices demonstrated μ_{elect} and μ_{hole} both $\sim 3 \times 10^{-2} \text{ cm}^2 \text{ V}^{-1} \text{ s}^{-1}$. Such a substance, with even, ambipolar charge transport, could be used to produce complementary inverters or light-emitting OTFTs.

Another way to modify the OTFT characteristics is to deposit a thin layer on top of the active layer. One group tested two metal oxides (lead oxide (PbO) and molybdenum oxide (MoO_3)) deposited on top of CuPc and F_{16}CuPc active layers in an OTFTs. They found that PbO deposited on CuPc and MoO_3 deposited on F_{16}CuPc produced devices— p -type and n -type, respectively—that operated in depletion mode.⁷¹ Generally, MPC transistors, including the other two combinations, operate in accumulation mode, so this is an interesting and alternative result. Another group deposited a 15 nm pentacene overlayer onto a F_{16}CuPc OTFT, and found that it decreased the value of V_T from 20.6 V to 0.53 V, compared to a control device, while also decreasing the μ_{elect} and $I_{\text{ON}}/I_{\text{OFF}}$.⁷²

■ PROCESSING OF MPCs

There are two methods that are most often used for the formation of MPC films within a OTFT: solution processing and thermal vapor deposition. Since most unmodified MPCs are insoluble, their films are generally deposited on a substrate in vacuum via thermal vapor deposition. Solution-processable MPCs, on the other hand, are typically spin-coated onto the substrate. Either sort of film may be heat-treated after formation, using a process called thermal annealing. Film properties of solution-processed MPCs are affected by concentration, solvent boiling point, and flow rate, while vacuum-deposited MPCs are affected by substrate temperature and deposition rate. These parameters directly affect the film morphology and, in turn, the electronic properties of the OTFTs that use them. This section summarizes the findings of various studies on the effect of these processing parameters on MPC-based OTFT performance.

As an example of thermal vapor deposition processing, Sinha et al. systematically studied the fabrication of CuPc-based OTFTs by maintaining the substrate temperature during CuPc deposition at 40, 80, and $120 \text{ }^\circ\text{C}$ and using OTS, poly(styrene), a polyimide complex (PIC), or untreated SiO_2 as the substrate for CuPc deposition.⁷³ The greatest μ value, $0.090 \text{ cm}^2 \text{ V}^{-1} \text{ s}^{-1}$, was obtained when using OTS-treated Si/SiO_2 and a substrate temperature of $80 \text{ }^\circ\text{C}$ during deposition.⁷³ A recent study even showed that the pressure during deposition also plays a role in the morphology of the CuPc film grown and correlates it to OTFT device characteristics.⁷⁴

Annealing at high temperature after vacuum deposition allows the molecules in the film to rearrange themselves, potentially improving/affecting/changing the film's electrical properties. For CuPc films deposited on ODTs-treated SiO_2 , increasing the annealing temperature increased the μ value for OTFT up to a temperature of $\sim 120 \text{ }^\circ\text{C}$, after which point it decreased.⁶⁴ The authors used grazing-incidence small-angle X-ray scattering to show that, above $150 \text{ }^\circ\text{C}$, the ODTs layer began to degrade and large islands of CuPc would form with high surface roughness. The performance of ZnPc transistors using a parylene-C insulating layer also increased after annealing at $120 \text{ }^\circ\text{C}$ for 3 h, with the field-effect μ value changing from $2.5 \times 10^{-2} \text{ cm}^2 \text{ V}^{-1} \text{ s}^{-1}$ to $3.7 \times 10^{-2} \text{ cm}^2 \text{ V}^{-1} \text{ s}^{-1}$.⁷⁵ The authors of that study calculated a 24% decrease in trap density after annealing that they attributed to the removal of oxygen impurities. They also noted an increase in grain size that they did not quantify.

The orientation of the π -stacking axis of MPCs directly affects the electronic properties of their films, which are innately anisotropic. Indeed, for MPC-based OTFTs, it is desirable to have the conduction occur parallel to the substrate. Besides

using an inducing layer such as ODTs, it is possible to affect this orientation by varying the processing conditions. Friedman et al. found that depositing CuPc onto SiO₂ at 300 °C produced grain growth parallel to the substrate, while depositing the CuPc at room temperature and then annealing at 300 °C produced grain growth perpendicular to the substrate.⁷⁶ The latter case had a superior μ value of $1.9 \times 10^{-3} \text{ cm}^2 \text{ V}^{-1} \text{ s}^{-1}$ and $I_{\text{ON}}/I_{\text{OFF}} = 1200$, compared to the former case with a μ value of $1.1 \times 10^{-4} \text{ cm}^2 \text{ V}^{-1} \text{ s}^{-1}$ and $I_{\text{ON}}/I_{\text{OFF}} = 270$. The authors suggest that one explanation for this observation could be that, for CuPc deposited on bare SiO₂, the π -stacking direction is perpendicular to the direction of grain growth. However, at least one study suggests that this is not always the case, proposing CuPc nanowire growth on SiO₂ is in the direction of π - π interactions.⁷⁷

The substrate temperature during deposition used in most studies for MPCs rarely exceeds 200 °C, so the superiority of annealing may not generally hold true. Many OTFTs show excellent performance when deposited at a high temperature or a slow rate without annealing. In one study, top-contact OTFTs were produced by depositing CuPc on a SiO₂ insulating layer at both 21 and 127 °C.⁶⁵ They found that increasing the deposition temperature increased the value of μ from $(1.5 \pm 0.6) \times 10^{-3} \text{ cm}^2 \text{ V}^{-1} \text{ s}^{-1}$ to $(6.5 \pm 0.8) \times 10^{-3} \text{ cm}^2 \text{ V}^{-1} \text{ s}^{-1}$, and again observed anisotropic grain growth parallel to the substrate. Sethuraman et al. found that F₁₆CuPc formed the most crystalline films with the highest μ value when deposited on a polycarbonate dielectric at 125 °C, as opposed to all other lower temperatures tested.⁷⁸ Similar to other cited authors, they suggest this performance increase is due to a decreased number of grain boundaries that form in the film when deposited at high temperature, thus decreasing the concentration of trap states and contact resistance.

The contact resistance plays a significant role in the overall device performance and has been reported to vary significantly, depending on the device configuration and processing conditions. For example, the typical contact resistance when using F₁₆CuPc is $\sim 1 \times 10^6 \Omega$; however, this resistance can be reduced to $\sim 4 \times 10^5 \Omega$ when using soft lamination techniques, where the bonding between the organic semiconductor and the metal electrodes and the organic semiconductor layer is formed by van der Waals forces.⁷⁹ Li et al. reported a drop in contact resistance from $\sim (2-4) \times 10^8 \Omega$ to $\sim (1-2) \times 10^7 \Omega$ for CuPc bottom-contact (BGBC) OTFTs when treating the electrodes with UV/ozone prior to CuPc deposition.⁸⁰ CuPc has even been used as a buffer layer between the gold electrodes and a pentacene semiconducting layer in a top-contact (BGTC), resulting in a reduction in contact resistance and an overall improvement in device performance.⁸¹

This resistance between the source-drain contacts and the organic film can be caused by physical irregularities on the surface of the film due to grain boundaries. Ghosh et al. found that increasing the substrate temperature to 100 °C and decreasing the deposition rate to 0.1 Å/s during vacuum deposition of F₁₆CuPc and CuPc increased the elongation of grains in the MPC films and increased the μ value of OTFTs by approximately an order of magnitude.⁸² They suggested that slower film-forming rates combined with higher molecular diffusion rates at higher temperature allowed the MPCs to produce larger crystals with fewer grain boundaries and, therefore, a better interface for the gold contacts.

Annealing (thermal treatment of the substrate and MPC layer together) can be used to improve the film quality of solution-

processable MPCs. OTFTs produced from the solubilized CuPc derivative (9, Figure 5) were annealed at various temperatures (room temperature, 50 °C, 100 °C, 150 °C, 200 °C) and the highest μ value of $0.7 \text{ cm}^2 \text{ V}^{-1} \text{ s}^{-1}$ was achieved for 100 °C.⁴⁰ The roughness of the CuPc film as determined using AFM was lowest at 1.6 nm for this temperature, while the average grain size (62 nm) as determined using XRD was highest. At higher temperatures, the surface roughness began to increase with crystallite size. The authors claimed that the smaller, elongated crystals that formed at lower temperatures showed better connectivity, behaving in a manner similar to a single crystal, in terms of the effects of trap states, despite being truly polycrystalline.

The change in morphology on annealing and OTFT performance has been investigated for other solution-processable MPCs as well. For the ZnPc, 8 the annealing process decreased the surface roughness determined using AFM from 10.9 nm to 5.5 nm, creating what appeared to be a more continuous film.⁴⁷ The OTFT devices they tested, when annealed, had an increased $I_{\text{ON}}/I_{\text{OFF}}$ value (from 10^3 to 10^4), a decreased V_T value (from 11 V to 3 V) and a smaller gate voltage dependence on μ . A bay-substituted (C₈H₁₇)₁₆ LuPc₂ derivative was shown to be a thermotropic liquid crystal with a mesophase transition at 62 °C, which makes relatively low temperature annealing possible.⁴³ AFM imagery revealed that films annealed at 70 °C, as opposed to room temperature, had a decreased surface roughness (2.2 nm, instead of 30 nm) and formed 150–200 nm clusters instead of 50–100 nm disks. OTFT devices with annealed films performed better across the board, with an increase in μ (from $1.5 \times 10^{-3} \text{ cm}^2 \text{ V}^{-1} \text{ s}^{-1}$ to $8 \times 10^{-3} \text{ cm}^2 \text{ V}^{-1} \text{ s}^{-1}$), an increase in $I_{\text{ON}}/I_{\text{OFF}}$ (from 10^3 to 10^5), a decrease in V_T (from -25 V to -12.5 V), and a decrease in grain-boundary density.

For some solution-processable MPCs, annealing does not substantially improve OTFT device performance. MPCs 1 and 2 (Figure 3) demonstrated μ increases of only 4% and 25% (to $0.96 \text{ cm}^2 \text{ V}^{-1} \text{ s}^{-1}$ and $0.4 \text{ cm}^2 \text{ V}^{-1} \text{ s}^{-1}$), respectively, when annealed at 80 and 120 °C, respectively.³⁹ The authors suggest that the specific peripheral substitution pattern of the alkyl constituents leads to room-temperature self-assembly and a high-quality film without annealing. Removing this step from the production of OTFTs could make their manufacture less complex and expensive; thus, this is a promising result.

The majority of MPC-based OTFTs use doped silicon as the gate contact and thermally grown SiO₂ between 150 and 400 nm as the gate insulator. Although there is some indication that CuPc grains grown on the oxide of *n*-doped silicon are laterally larger and vertically smaller, producing rougher, more open films than those grown on the oxide of *p*-doped silicon,⁸³ there have been no studies done on whether the gate doping affects films grown on inducing layers or for MPCs other than CuPc. Many studies use either or do not specify the doping type. In this section, gate and insulating layers other than Si/SiO₂ that have been used for MPC-based OTFTs will be discussed, including their potential effects on device properties.

■ THE GATE AND INSULATING/DIELECTRIC LAYER

One reason to explore the use of other insulating layers is because SiO₂ has a relatively low dielectric constant ($\epsilon_r \approx 3.9$).⁸⁴ Insulating layers with higher dielectric constants are easier to polarize, and thus a smaller gate voltage is required to turn on the transistors that use them. In addition, such OTFTs may have reduced leakage currents and potentially higher $I_{\text{ON}}/$

I_{OFF} ratios. Huth et al. found that utilizing SrTiO₃ as the insulating layer ($\epsilon_r = 300$) with Nb-doped SrTiO₃ as the gate produced CuPc transistors with $I_{\text{ON}}/I_{\text{OFF}}$ ratios as high as 10^3 and a V_T value as low as 0.27 V.⁸⁵ The μ value for the CuPc active layer was only $1.5 \times 10^{-3} \text{ cm}^2 \text{ V}^{-1} \text{ s}^{-1}$, but no inducing layer was used to improve the CuPc film itself. Bottom-contact CuPc OTFTs using 22 nm HfO₂ or HfAlO as gate insulators on etched silicon had a V_T value of less than -2 V and $I_{\text{ON}}/I_{\text{OFF}}$ ratios of $\sim 10^3$.⁸⁶ This study found that the type of gate insulator did affect the CuPc film properties, with HfAlO producing 66% larger grains, 31% lower defect density, and 20% less roughness, compared to HfO₂, as measured using AFM. In turn, the former had a μ value of $2.6 \times 10^{-3} \text{ cm}^2 \text{ V}^{-1} \text{ s}^{-1}$, compared to $1.6 \times 10^{-3} \text{ cm}^2 \text{ V}^{-1} \text{ s}^{-1}$ for the latter.

Silicon nitride has also been investigated as a potential gate dielectric insulator for MPc OTFTs. Yan et al. fabricated OTFTs with an Al/Nd alloy for the gate, silicon nitride (SiN_x) for the gate insulator, VOPc for the active layer, and gold for the source/drain contacts.^{87,88} These devices showed a maximum μ value of $1.4 \text{ cm}^2 \text{ V}^{-1} \text{ s}^{-1}$ and $V_T = -4.22 \text{ V}$, the latter varying by $<1 \text{ V}$ under temperature stress (100 °C) under vacuum and gate bias stress (-20 V) in air.⁸⁸ The authors attributed this stability to the SiN_x gate dielectric, which may form a low-defect interface with VOPc. They also found the devices could operate with high frequency, low series resistance, and small hysteresis.⁸⁷

Polymers may be useful for gate insulators in OTFTs, because of their mechanical flexibility. Monochlorinated poly(parylene), parylene-C (Figure 8), was used as the

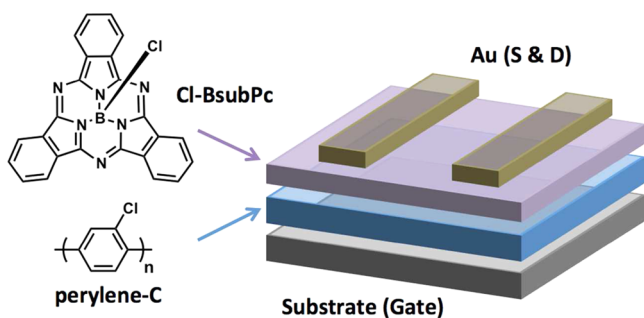


Figure 8. Structure of a bottom-gate, top-contact OTFT using parylene-C as the insulating layer and chloro boron subphthalocyanine (Cl-BsubPc) as the semiconductive MPc layer.

insulator for chloro boron subphthalocyanine⁸⁹ (Cl-BsubPc, Figure 8) transistors (insulator thickness of $\sim 1000 \text{ nm}$) that achieved μ_{elect} values as high as $5.4 \times 10^{-5} \text{ cm}^2 \text{ V}^{-1} \text{ s}^{-1}$,³⁷ while magnesium MPc (MgPc) transistors (insulator thickness of $\sim 490 \text{ nm}$) achieved a μ_{hole} value of $0.021 \text{ cm}^2 \text{ V}^{-1} \text{ s}^{-1}$,³³ and ZnPc transistors (insulator thickness of $\sim 490 \text{ nm}$) achieved a μ_{hole} value as high as $0.037 \text{ cm}^2 \text{ V}^{-1} \text{ s}^{-1}$.⁷⁵

Sethuraman et al. demonstrated viable use of a polycarbonate gate insulator (thickness of $\sim 950 \text{ nm}$) when they produced *n*-type OTFTs using F₁₆CuPc with μ values as high as $6.0 \times 10^{-3} \text{ cm}^2 \text{ V}^{-1} \text{ s}^{-1}$.⁷⁸ Finally, the OTFTs mentioned earlier, that were made with dimeric ZnPc and CoPc and had μ_{hole} values of $2.8 \times 10^{-3} \text{ cm}^2 \text{ V}^{-1} \text{ s}^{-1}$ and $7.3 \times 10^{-3} \text{ cm}^2 \text{ V}^{-1} \text{ s}^{-1}$, respectively, used a poly(vinyl alcohol) (PVA) insulator with a thickness of 300 nm .⁵⁰

A more exotic example of a gate insulator is an ionic liquid that separates the active layer from the gate. Figure 9 shows the structure of a top-gate, bottom-contact OTFT with an ionic

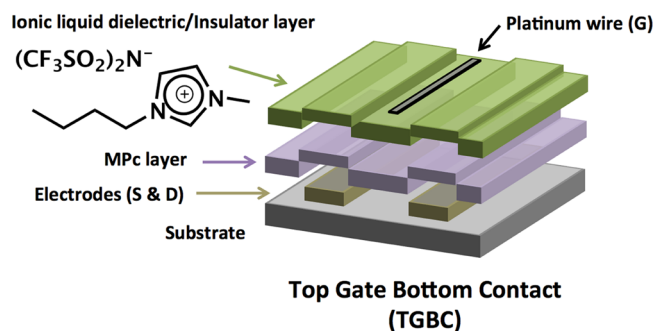


Figure 9. Structure of a top-gate, bottom-contact OTFT using an ionic liquid as the gate insulator.

liquid as the gate insulator. Devices using PbPc and TiOPc as the active layer and various ionic liquids were mostly ambipolar with extremely low V_T values, because of the high capacitances of the ionic liquids.³⁴ The PbPc device with 1-butyl-3-methylimidazolium bis(trifluoromethylsulfonyl)imide (BMIM-TFSI, Figure 9) as the ionic liquid, for example, had a V_T value of 0.25 V for holes and 1.52 V for electrons. OTFTs fabricated using PbPc were characterized by having $\mu_{\text{elect}} = 10^{-3} \text{ cm}^2 \text{ V}^{-1} \text{ s}^{-1}$ and $\mu_{\text{hole}} = 10^{-2} \text{ cm}^2 \text{ V}^{-1} \text{ s}^{-1}$, while those made with TiOPc were characterized by having $\mu_{\text{elect}} = \mu_{\text{hole}} = 10^{-3} \text{ cm}^2 \text{ V}^{-1} \text{ s}^{-1}$. Given the top-gate configuration of the device, it would be difficult to utilize an inducing layer to improve μ .

Source-Drain Contacts. The configuration of the source-drain (SD) contacts is commonly varied in OTFT literature, with the electrodes either deposited on top of the organic film (top contact) or the organic film deposited on top of the electrodes (bottom contact). Gold is predominantly used for the contact material in MPc OTFTs, although other high-work-function metals, such as silver⁶⁹ or platinum,^{34,38} are occasionally used as well. This section will focus on the gold/MPc interface and a few other contact materials that have been used in MPc-based OTFTs.

The energetics of electron and hole barriers at interfaces are complex. Despite having a similar work function ($\sim 5 \text{ eV}$) to the HOMO energy of CuPc but not the LUMO, top-contact CuPc devices with gold SD contacts can demonstrate ambipolar charge transport.⁶⁹ In the same study, devices with high-work-function organic metals, such as TSF/F₂TXNQ (20/21, Figure 10), demonstrated only a *p*-type field effect, but had a lower

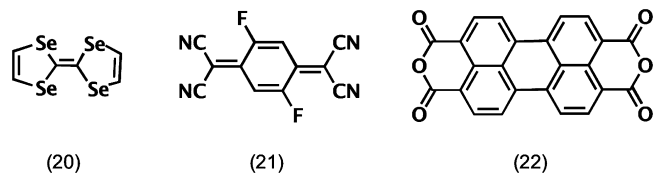


Figure 10. Structures of TSF (20), F₂TXNQ (21), and PTCDA (22).

calculated contact resistance. One explanation offered was that the Fermi level of gold shifts closer to the vacuum, between the HOMO and LUMO of CuPc. Certainly, clusters of deposited gold may diffuse into the CuPc film during deposition, with both the Au 6s states and CuPc HOMO level shifting toward the Fermi level.⁹⁰ This interaction may include charge transfer from the organic layer into the gold contacts.⁹¹ Silver, on the other hand, forms an abrupt, inert interface when deposited on CuPc,⁹² demonstrating that it may be a better material for top

contacts if its work function is sufficiently high for efficient hole transfer.

The injection barrier, or energetic difference between electrode work function and LUMO (for electrons) or HOMO (for holes) is often cited as a cause for nonideal charge transport characteristics in OTFTs. Tsutsui et al. produced top-contact transistors using chloro boron subphthalocyanine (Cl-BsubPc, Figure 8) that achieved $\mu_{\text{elect}} = 5.4 \times 10^{-5} \text{ cm}^2 \text{ V}^{-1} \text{ s}^{-1}$ using low-work-function calcium SD contacts and $\mu_{\text{elect}} = 1.2 \times 10^{-5} \text{ cm}^2 \text{ V}^{-1} \text{ s}^{-1}$ for high-work-function gold SD contacts. They found that the gold contact device operated in *p*-mode after exposure to air and attributed the difference in μ to the lower electron injection barrier between calcium and BsubPc.³⁷ Carbon nanotubes (CNTs) have also been used for SD contacts in CuPc devices.⁹³ Bottom-contact OTFTs made in this study had a μ_{hole} value of $1.2 \times 10^{-2} \text{ cm}^2 \text{ V}^{-1} \text{ s}^{-1}$ using CNT and $\mu_{\text{hole}} = 5 \times 10^{-3} \text{ cm}^2 \text{ V}^{-1} \text{ s}^{-1}$ using gold electrodes, with $I_{\text{ON}}/I_{\text{OFF}}$ ratios of 10^6 and 10^3 , respectively. The authors found that the devices with gold contacts were ambipolar, while the CNT devices were *p*-type before annealing and ambipolar after annealing for 24 h. CNT devices demonstrated ohmic (linear) resistance at low voltages for both holes and electrons, while gold devices did not, indicating a superior contact. The authors suggested that the ohmic contact during electron transport, despite a high energy barrier between the work function of CNT and LUMO of CuPc, indicates that electron tunnelling is responsible for charge transfer between the contacts.

■ APPLICATIONS OF MPC-BASED OTFTS

OTFTs have been proposed for integration into applications such as flexible circuits, radio frequency identification (RFID) tags, and sensors. Recent literature for MPC-based OTFTs indicates their potential use in light sensors,^{36,94–97} chemical noses,^{98,99} radiation detectors,¹⁰⁰ as well as electronic inverters⁷⁷ and neural circuit simulators.¹⁰¹

Palladium phthalocyanine (PdPc) has been used for photoresponsive organic field-effect transistors (PhOFETs), which switch on under illumination, as opposed to increased gate voltage. Peng et al. used the bilayer structure shown in Figure 11, incorporating a fullerene (C_{60}) layer to promote

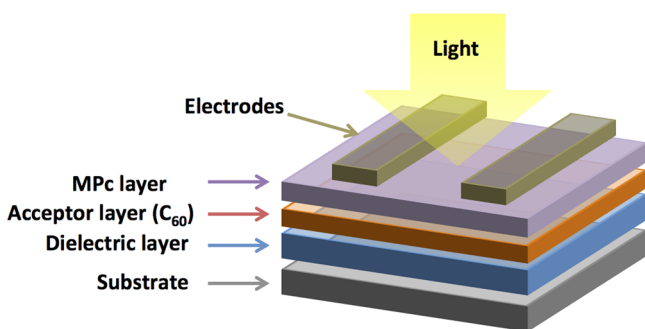


Figure 11. Photoresponsive organic field-effect transistor (PhOFET) diagram with a bilayer structure.

photogenerated exciton dissociation at the junction between PdPc and C_{60} .³⁶ They achieved a photosensitivity of 8×10^3 and a photoresponsivity of 28.2 mA/W for an optimal architecture, where PdPc was placed above the C_{60} layer and touching the gold contacts (see Figure 11). The authors justified the use of PdPc because it is reported to have a higher

exciton diffusion length than CuPc or ZnPc.^{102,103} The same group found that using aluminum contacts instead of gold contacts could significantly increase the photosensitivity by decreasing the background dark current.⁹⁴ They postulated this decrease was due to the increased barrier for hole injection from the mismatch between the work function of the SD contact metal and the HOMO of PdPc. In addition, they found that the photosensitivity and photoresponsivity of these devices both increased as the gate voltage increased, which is a phenomenon not observed when gold contacts were used.

Photoresponsivity has also been demonstrated in various devices incorporating other MPCs. One PhOFET using CuPc as the donor and PTCDA (21, Figure 10) as the acceptor layer was produced, demonstrating a major shift in V_T for hole conduction of ~ 16 V on illumination.⁹⁵ Vertical structure thin-film transistors demonstrated a factor of 2.9–6.4 increase in current when illuminated with white light.⁹⁷ Top-contact lead PdPc OTFTs transformed from *p*-type to ambipolar upon illumination, with almost-balanced $\mu_{\text{hole}} = 3.0 \times 10^{-5} \text{ cm}^2 \text{ V}^{-1} \text{ s}^{-1}$ and $\mu_{\text{elect}} = 1.8 \times 10^{-5} \text{ cm}^2 \text{ V}^{-1} \text{ s}^{-1}$.¹⁰⁴ Even inorganic photoresponsive OTFTs can benefit from the incorporation of a CuPc layer, because of its high absorptivity. Zhang et al. produced InGaZnO OTFTs with a CuPc light absorption layer and found that it increased the photoresponsivity of the device by a factor of 5.⁹⁶ This highlights the versatility of MPC compounds in optical devices.

Wood et al. incorporated a charge-retaining architecture below the active layer of a transistor to induce a semipermanent retention of the device's $I_{\text{ON}}/I_{\text{OFF}}$ status. The authors fabricated a SONOS ($\text{SiO}_2/\text{SiN}/\text{SiO}_2$) layer sequence above the gate in a CuPc transistor, as a proof-of-concept design to simulate neural spiking.¹⁰¹ In this case, amorphous CuPc provided a well-studied material that the authors claimed could be incorporated into stacked, three-dimensional (3D) circuits with high interconnectivity.

In order to utilize OTFTs for more-advanced devices, it is essential to develop basic electronic components, such as inverters. Essentially, an inverter produces a high voltage output (V_{OUT}) when the input voltage (V_{IN}) is low and vice versa. One study found complementary CuPc and F_{16}CuPc deposited at 100°C on Si/SiO_2 had similar μ_{hole} and μ_{elect} values, of $1.5 \times 10^{-2} \text{ cm}^2 \text{ V}^{-1} \text{ s}^{-1}$ and $1.8 \times 10^{-2} \text{ cm}^2 \text{ V}^{-1} \text{ s}^{-1}$, respectively.⁷⁷ The authors also successfully incorporated these MPCs in the fabrication of the organic inverter. They argued that using CuPc and F_{16}CuPc , which have similar HOMO and LUMO levels, respectively, allows the use of a single gate electrode (gold), thus simplifying the design of the device.

MPC-based OTFTs have even been used for gas detection sensors (see Figure 12).¹⁰⁵ The analytes either interact with the surface through molecular bonding or diffuse into the organic layer, resulting in a change in μ (see Figure 12). Recently, Zhang et al. used a CuPc OTFT to detect H_2S gas in dry air.⁹⁹ They proposed that, when the concentration of H_2S increases, the oxygen adsorbed on the surface of the MPC film is displaced by H_2S molecules. The reducing gas injects electrons into the *p*-type material, eliminating holes and decreasing current between the source and the drain. The authors tested the specificity of the sensor and found a moderate response to SO_2 and a minor response to CH_4 , H_2 , and CO_2 . In order to increase the variety of analytes that can be detected, Katz et al. combined the CuPc transistor with two other organic transistors.⁹⁸ This array could be used to distinguish eight analytes, including water, acetone, hexane, hydrogen peroxide, and toluene, by analyzing the

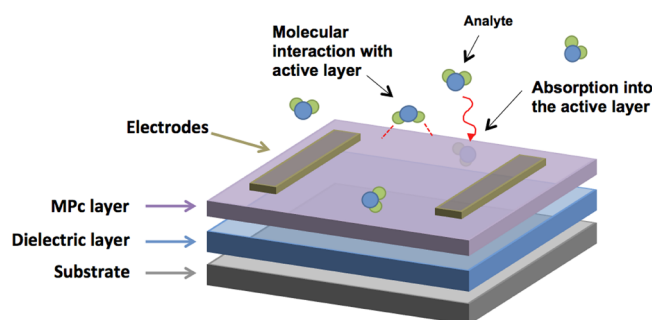


Figure 12. Gas sensors based on OTFT diagram with two potential modes of interaction between the organic layer and the analyte.

direction and magnitude of response for each OTFT upon exposure.

Another possible application of CuPc is for radiation dosimetry. Rao et al. determined that γ radiation induces *p*-doping in CuPc films, decreasing the resistance in thin films and increasing the off current in encapsulated OTFTs.¹⁰⁰ In order to magnify these changes, they connected the transistors in parallel, in order to increase the off current both before and after irradiation, increasing the magnitude of the difference. The previously mentioned encapsulation layer was composed of SiN, which prevented significant electronic changes caused by gases in the atmosphere, such as H₂S, which are known to affect CuPc OTFTs. The net effect of irradiation was found to be permanent within 48 h, suggesting such devices would provide a good measure of cumulative exposure.

OUTLOOK

In our view, the ongoing development of new MPc-based OTFTs can be divided into two general categories: (i) the synthesis and introduction of new MPc derivatives into OTFTs and (ii) the optimization and device engineering of OTFTs using more common but still understudied MPcs. The latter category can be further subdivided based on intent. Given that the best MPc-based OTFTs have μ values of up to 1.0–10.0 cm² V⁻¹ s⁻¹, comparable to devices using pentacene and other high-performance organic semiconductors,^{1–3,5–9} the optimization of device parameters such as μ , I_{ON}/I_{OFF} ratio, and V_T continues to be warranted. On the other hand, with the potential for unannealed, solution-processable devices that demonstrate good performance,³⁹ serious research into low-cost MPc-TFT production is also important. Finally, specific applications such as photosensitive transistors, flexible transistors, and sensors should continue to be studied and optimized if commercialization is the end goal.

There are many metalloids, metals, and metal oxides that have not yet been tested as the central metal/component of a MPc in the active layer of a thin-film transistor, such as silver,¹⁰⁶ sodium,³⁸ or silicon. Given the large variety in electrical properties for the various MPcs in OTFTs, any of these materials, although they would have to be synthesized in house, could be high-performing with the right inducing layer or processing conditions, and could be further modified with solubilizing groups. Solution-processed MPcs generally are important, in that they may be the best candidates for low-cost or large-scale applications where vacuum deposition might be more difficult or expensive. Certainly, the few published studies that have utilized these MPcs in OTFTs have produced some excellent results, with μ values as high as ~ 1 cm² V⁻¹ s⁻¹, high

I_{ON}/I_{OFF} ratios and a low V_T , some with no or low-temperature annealing, which could further reduce cost. Despite these reports, research in this area is still behind that of vacuum-deposited MPcs, in terms of the variety of central atoms, presence and type of inducing layers, and type of insulating layer. Successful substituent attachment patterns should be tested on other promising MPc candidates, such as the *n*-type TiOPc.^{28,30} Many soluble MPc derivatives have been synthesized and studied but not in transistors.^{107,108} Only after more data have been collected will we have a better idea of the best solution-processable MPcs and their device properties.

Performance tuning using annealing or inducing layers must be further investigated for the different types of MPcs as well. Indeed, it is important to understand how these modifications can affect the crystal growth, charge transport, and device properties of each type of MPcs and its soluble derivatives. Despite the structural similarity of many MPcs, electronic variations caused by changes in the central atom or peripheral substitution still require careful investigations. Currently, it seems that different compounds used for inducing layers produce different results, depending on the MPc, and the optimal thickness and processing of these layers may also vary. The vast majority of soluble MPcs in OTFTs use silanes (ODTS, OTS, PTS) for the inducing layer, which are not usually the best performers for insoluble MPcs. It is possible that improved device performance could be achieved by trying alternative compatible materials.

Overall, it is the opinion of the authors that MPc are generally good candidates for OTFTs and other organic electronic devices. MPcs are relatively simple and inexpensive to synthesize in large amounts (kilogram scale) and are easily chemically modified to suit all processing needs and final device configuration. In addition, their adoption as pigments and xerographic materials by several major industrial research groups such as Xerox Corporation, Canon, Inc., and Lexmark International, Inc. is evidence that these molecules show promise. However, there is much work that can and should be done if the potential of MPc-based OTFTs is to be fully realized. The stability, ease of manufacture, and electronic and film-forming properties of the MPcs make them attractive candidates for not just thin-film transistors but also photovoltaics^{103,109–113} and other organic electronic applications such as sensors and light-emitting diodes. With such a wealth of available but unproven MPcs structural variants, systematic investigations of each is certainly warranted.

AUTHOR INFORMATION

Corresponding Authors

*E-mail: benoit.lessard@uottowa.ca (B. H. Lessard).

*E-mail: tim.bender@utoronto.ca (T. P. Bender).

Notes

The authors declare no competing financial interest.

REFERENCES

- (1) Newman, C. R.; Frisbie, C. D.; da Silva Filho, D. A.; Brédas, J.-L.; Ewbank, P. C.; Mann, K. R. Introduction to Organic Thin Film Transistors and Design of *n*-Channel Organic Semiconductors. *Chem. Mater.* **2004**, *16*, 4436–4451.
- (2) Roberts, M. E.; Sokolov, A. N.; Bao, Z. Material and Device Considerations for Organic Thin-Film Transistor Sensors. *J. Mater. Chem.* **2009**, *19*, 3351–3363.
- (3) Wen, Y.; Liu, Y. Recent Progress in *n*-Channel Organic Thin-Film Transistors. *Adv. Mater.* **2010**, *22*, 1331–1345.

- (4) Horowitz, G. Organic Thin Film Transistors: From Theory to Real Devices. *J. Mater. Res.* **2004**, *19*, 1946–1962.
- (5) DiBenedetto, S. A.; Facchetti, A.; Ratner, M. A.; Marks, T. J. Molecular Self-Assembled Monolayers and Multilayers for Organic and Unconventional Inorganic Thin-Film Transistor Applications. *Adv. Mater.* **2009**, *21*, 1407–1433.
- (6) Dimitrakopoulos, C. D.; Mascaro, D. J. Organic Thin-Film Transistors: A Review of Recent Advances. *IBM J. Res. Dev.* **2001**, *45*, 11–27.
- (7) Dimitrakopoulos, C. D.; Malenfant, P. R. L. Organic Thin Film Transistors for Large Area Electronics. *Adv. Mater.* **2002**, *14*, 99–117.
- (8) Li, L.; Tang, Q.; Li, H.; Hu, W.; Yang, X.; Shuai, Z.; Liu, Y.; Zhu, D. Organic Thin-Film Transistors of Phthalocyanines. *Pure Appl. Chem.* **2008**, *80*, 2231–2240.
- (9) Ling, M. M.; Bao, Z. Thin Film Deposition, Patterning, and Printing in Organic Thin Film Transistors. *Chem. Mater.* **2004**, *16*, 4824–4840.
- (10) Yuen, A. P.; Jovanovic, S. M.; Hor, A.-M.; Klenkler, R. A.; Devenyi, G. A.; Loutfy, R. O.; Preston, J. S. Photovoltaic Properties of M-phthalocyanine/Fullerene Organic Solar Cells. *Sol. Energy* **2012**, *86*, 1683–1688.
- (11) *Phthalocyanine Materials: Synthesis, Structure, and Function*; McKeown, N. B., Ed.; Cambridge University Press: Cambridge, U.K., 1998.
- (12) Dahlen, M. A. The Phthalocyanines A New Class of Synthetic Pigments and Dyes. *Ind. Eng. Chem.* **1939**, *31*, 839–847.
- (13) Claessens, C. G.; Hahn, U.; Torres, T. Phthalocyanines: From outstanding electronic properties to emerging applications. *Chem. Rec.* **2008**, *8*, 75–97.
- (14) de la Torre, G.; Claessens, C. G.; Torres, T. Phthalocyanines: Old Dyes, New Materials. Putting Color in Nanotechnology. *Chem. Commun.* **2007**, 2000–2015.
- (15) de la Torre, G.; Vazquez, P.; Agullo-Lopez, F.; Torres, T. Phthalocyanines and Related Compounds: Organic Targets for Nonlinear Optical Applications. *J. Mater. Chem.* **1998**, *8*, 1671–1683.
- (16) Branstion, R. E.; Duff, J. M. Photoresponsive Imaging Members with Dihydroxy Metal Phthalocyanine Compositions. U.S. Patent 4,557,989, Dec. 10, 1985.
- (17) Ong, B. S.; Bluhm, T. L.; Hsiao, C. K.; Duff, J. M. Hydroxygermanium Phthalocyanine Processes. U.S. Patent 5,441,837, Aug. 15, 1995.
- (18) Ong, B. S.; Hsiao, C. K. Photoconductive Imaging Members with Acetoxymetal Phthalocyanines. U.S. Patent 5,382,493, Jan. 17, 1995.
- (19) Ong, B. S.; Hsiao, C. K. Preparative Processes for Dihydroxygermanium Phthalocyanine. U.S. Patent 5,491,228, Feb. 13, 1996.
- (20) Borsenberger, P. M. *Organic Photoreceptors for Xerography*, Vol. 59; CRC Press: Boca Raton, FL, 1998.
- (21) Byrne, J. F. Electrophotographic Element Containing Phthalocyanine. U.S. Patent 3,816,118, June 11, 1974.
- (22) Titterington, D. R.; Meinhardt, M. B.; Banning, J. H.; Mayo, J. D.; Duff, J. M.; Gaynor, R. E.; Frame, H. R. Ink Compositions Containing Phthalocyanines. U.S. Patent 6,726,755, Apr. 27, 2004.
- (23) King, C. R.; Titterington, D. R.; Banning, J. H. Metal Phthalocyanine Colorants for Phase Change Inks. U.S. Patent 6,221,137, Apr. 24, 2001.
- (24) Bertrand, J. C.; Ciccirelli, R. N.; Pickering, T. R.; Bayley, D. R. Four Color Toner Set. U.S. Patent 5,620,820, Apr. 15, 1997.
- (25) Tsuji, I.; Tochihara, S.; Osumi, K.; Takuhara, H.; Kawabe, M.; Yamakami, H. Ink Jet Recording Ink, Ink Jet Recording Method, Ink Cartridge, and Ink Jet Recording Apparatus. U.S. Patent 7,244,299, Jul. 17, 2007.
- (26) Patel, P.; Horrobin, T. M. Phthalocyanine Compounds and Ink Compositions Comprising the Same. U.S. Patent 7,022,171, Apr. 4, 2006.
- (27) McKeown, N. B. *Phthalocyanine Materials: Synthesis, Structure, and Function*; Cambridge University Press: Cambridge, U.K., 1998.
- (28) Li, L.; Tang, Q.; Li, H.; Yang, X.; Hu, W.; Song, Y.; Shuai, Z.; Xu, W.; Liu, Y.; Zhu, D. An Ultra Closely π -Stacked Organic Semiconductor for High Performance Field-Effect Transistors. *Adv. Mater.* **2007**, *19*, 2613–2617.
- (29) Pan, F.; Tian, H.; Qian, X.; Huang, L.; Geng, Y.; Yan, D. High Performance Vanadyl Phthalocyanine Thin-Film Transistors Based on Fluorobenzene End-Capped Quaterthiophene as the Inducing Layer. *Org. Electron.* **2011**, *12*, 1358–1363.
- (30) Huang, L.; Yu, B.; Song, D.; Geng, Y.; Zhu, F.; Yan, D. Tin (IV) Phthalocyanine Oxide: An Air-Stable Semiconductor with High Electron Mobility. *Appl. Phys. Lett.* **2008**, *92*, 143303.
- (31) Wang, H.; Zhu, F.; Yang, J.; Geng, Y.; Yan, D. Weak Epitaxy Growth Affording High-Mobility Thin Films of Disk-Like Organic Semiconductors. *Adv. Mater.* **2007**, *19*, 2168–2171.
- (32) Gu, W.; Hu, Y.; Zhu, Z.; Liu, N.; Zhang, J.; Wang, J. Preparing Highly Ordered Copper Phthalocyanine Thin-Film by Controlling the Thickness of the Modified Layer and its Application in Organic Transistors. *Solid-State Electron.* **2013**, *89*, 101–104.
- (33) Rajesh, K. R.; Menon, C. S. Polymeric Gated Organic Field Effect Transistor Using Magnesium Phthalocyanine. *Proc. SPIE* **2014**, *9185*, 918515.
- (34) Fujimoto, T.; Matsushita, M. M.; Awaga, K. Ambipolar Carrier Injections Governed by Electrochemical Potentials of Ionic Liquids in Electric-Double-Layer Thin-Film Transistors of Lead- and Titanyl-Phthalocyanine. *J. Phys. Chem. C* **2013**, *117*, 5552–5557.
- (35) Bao, Z.; Lovinger, A. J.; Dodabalapur, A. Highly Ordered Vacuum-Deposited Thin Films of Metallophthalocyanines and Their Applications in Field-Effect Transistors. *Adv. Mater.* **1997**, *9*, 42–44.
- (36) Yao, B.; Peng, Y.; Gao, P.; Fan, G.; Lv, W.; Zhou, M.; Chen, D. Influence of Donor-Acceptor Layer Sequence on Photoresponsive Organic Field-Effect Transistors Based on Palladium Phthalocyanine and C₆₀. *Appl. Phys. Lett.* **2013**, *102*, 163303–163305.
- (37) Yasuda, T.; Tsutsui, T. *n*-Channel Organic Field-Effect Transistors Based on Boron-Subphthalocyanine. *Mol. Cryst. Liq. Cryst.* **2006**, *462*, 3–9.
- (38) Hasegawa, H. Fabrication of Sodium Phthalocyanine Nanocrystals Using Nanoscale Electrocrystallization. *New J. Chem.* **2013**, *37*, 2271–2274.
- (39) Dong, S.; Bao, C.; Tian, H.; Yan, D.; Geng, Y.; Wang, F. ABAB-Symmetric Tetraalkyl Titanyl Phthalocyanines for Solution Processed Organic Field-Effect Transistors with Mobility Approaching 1 cm² V⁻¹ s⁻¹. *Adv. Mater.* **2013**, *25*, 1165.
- (40) Chaure, N. B.; Pal, C.; Barard, S.; Kreouzis, T.; Ray, A. K.; Cammidge, A. N.; Chambrier, I.; Cook, M. J.; Murphy, C. E.; Cain, M. G. A Liquid Crystalline Copper Phthalocyanine Derivative for High Performance Organic Thin Film Transistors. *J. Mater. Chem.* **2012**, *22*, 19179–19189.
- (41) Chaidogiannos, G.; Petraki, F.; Glezos, N.; Kennou, S.; Nešpůrek, S. Low Voltage Operating OFETs Based on Solution-Processed Metal Phthalocyanines. *Appl. Phys. A: Mater. Sci. Process.* **2009**, *96*, 763–767.
- (42) Kong, X.; Zhang, X.; Gao, D.; Qi, D.; Chen, Y.; Jiang, J. Air-Stable Ambipolar Field-Effect Transistor Based on a Solution-Processed Octanaphthoxy-Substituted Tris(Phthalocyaninato) Europium Semiconductor with High and Balanced Carrier Mobilities. *Chem. Sci.* **2015**, *6*, 1967–1972.
- (43) Chaure, N. B.; Sosa-Sanchez, J. L.; Cammidge, A. N.; Cook, M. J.; Ray, A. K. Solution Processable Lutetium Phthalocyanine Organic Field-Effect Transistors. *Org. Electron.* **2010**, *11*, 434–438.
- (44) Dong, S.; Tian, H.; Song, D.; Yang, Z.; Yan, D.; Geng, Y.; Wang, F. The First Liquid Crystalline Phthalocyanine Derivative Capable of Edge-on Alignment for Solution Processed Organic Thin-Film Transistors. *Chem. Commun.* **2009**, 3086–3088.
- (45) Dong, S.; Tian, H.; Huang, L.; Zhang, J.; Yan, D.; Geng, Y.; Wang, F. Non-peripheral Tetrahexyl-Substituted Vanadyl Phthalocyanines with Intermolecular Cofacial π - π stacking for Solution-Processed Organic Field-Effect Transistors. *Adv. Mater.* **2011**, *23*, 2850–2854.

- (46) Jiménez Tejada, J. A.; Awawdeh, K. M.; Villanueva, J. A. L.; Carceller, J. E.; Deen, M. J.; Chaure, N. B.; Basova, T.; Ray, A. K. Contact Effects in Compact Models of Organic Thin Film Transistors: Application to Zinc Phthalocyanine-Based Transistors. *Org. Electron.* **2011**, *12*, 832–842.
- (47) Faris, T.; Basova, T.; Chaure, N. B.; Sharma, A. K.; Durmuş, M.; Ahsen, V.; Ray, A. K. Effects of Annealing on Device Parameters of Organic Field Effect Transistors using Liquid-Crystalline Tetrasubstituted Zinc Phthalocyanine. *EPL* **2014**, *106*, 58002.
- (48) Sharma, A.; Zahedi, M.; Durmuş, M.; Basova, T.; Ray, A.; Ahsen, V.; Chaure, N. Solution Processed Tetrasubstituted Zinc Phthalocyanine as an Active Layer in Organic Field Effect Transistors. *J. Appl. Phys.* **2010**, *107*, 114503.
- (49) Chaure, N. B.; Camidge, A. N.; Chambrier, I.; Cook, M. J.; Cain, M. G.; Murphy, C. E.; Pal, C.; Ray, A. K. High-mobility Solution-Processed Copper Phthalocyanine-Based Organic Field-Effect Transistors. *Sci. Technol. Adv. Mater.* **2011**, *12*, 025001.
- (50) Özer, L. M.; Özer, M.; Altındal, A.; Özkaya, A. R.; Salih, B.; Bekaroğlu, Ö. Synthesis, Characterization, OFET and Electrochemical Properties of Novel Dimeric Metallophthalocyanines. *Dalton Trans.* **2013**, *42*, 6633–6644.
- (51) Li, D.; Wang, H.; Kan, J.; Lu, W.; Chen, Y.; Jiang, J. H-aggregation Mode in Triple-Decker Phthalocyaninato-Europium Semiconductors. Materials Design for High-Performance Air-Stable Ambipolar Organic Thin Film Transistors. *Org. Electron.* **2013**, *14*, 2582–2589.
- (52) Kong, X.; Jia, Q.; Wu, F.; Chen, Y. Flexible, Ambipolar Organic Field-Effect Transistors Based on the Solution-Processed Films of Octanaphthoxy-Substituted Bis(Phthalocyaninato) Europium. *Dyes Pigm.* **2015**, *115*, 67–72.
- (53) Chen, Y.; Bouvet, M.; Sizun, T.; Gao, Y.; Plassard, C.; Lesniewska, E.; Jiang, J. Facile Approaches to Build Ordered Amphiphilic Tris(Phthalocyaninato) Europium Triple-Decker Complex thin Films and their Comparative Performances in Ozone Sensing. *Phys. Chem. Chem. Phys.* **2010**, *12*, 12851–12861.
- (54) Gao, D.; Zhang, X.; Kong, X.; Chen, Y.; Jiang, J. (TFPP)Eu-[Pc(OPh)₈]Eu[Pc(OPh)₈]/CuPc Two-Component Bilayer Heterojunction-Based Organic Transistors with High Ambipolar Performance. *ACS Appl. Mater. Interfaces* **2015**, *7*, 2486–2493.
- (55) Ma, P.; Kan, J.; Zhang, Y.; Hang, C.; Bian, Y.; Chen, Y.; Kobayashi, N.; Jiang, J. The First Solution-Processable n-Type Phthalocyaninato Copper Semiconductor: Tuning the Semiconducting Nature via Peripheral Electron-Withdrawing Octyloxycarbonyl Substituents. *J. Mater. Chem.* **2011**, *21*, 18552–18559.
- (56) Miyazaki, E.; Kaku, A.; Mori, H.; Iwatani, M.; Takimiya, K. S-Hexylthiophene-Fused Porphyrazines: New Soluble Phthalocyanines for Solution-Processed Organic Electronic Devices. *J. Mater. Chem.* **2009**, *19*, 5913–5915.
- (57) Chua, L.-L.; Zaumseil, J.; Chang, J.-F.; Ou, E. C. W.; Ho, P. K. H.; Sirringhaus, H.; Friend, R. H. General Observation of n-Type Field-Effect Behaviour in Organic Semiconductors. *Nature* **2005**, *434*, 194–199.
- (58) Puigdollers, J.; Voz, C.; Fonrodona, M.; Cheylan, S.; Stella, M.; Andreu, J.; Vetter, M.; Alcubilla, R. Copper Phthalocyanine Thin-Film Transistors with Polymeric Gate Dielectric. *J. Non-Cryst. Solids* **2006**, *352*, 1778–1782.
- (59) Shi, J.; Wang, H.; Song, D.; Tian, H.; Geng, Y.; Yan, D. Ambipolar Organic Heterojunction Transistors with Various p-Type Semiconductors. *Thin Solid Films* **2008**, *516*, 3270–3273.
- (60) Xiao, K.; Liu, Y.; Guo, Y.; Yu, G.; Wan, L.; Zhu, D. Influence of Self-Assembly Monolayers on the Characteristics of Copper Phthalocyanine Thin Film Transistor. *Appl. Phys. A: Mater. Sci. Process.* **2005**, *80*, 1541–1545.
- (61) Dong, H.; Fu, X.; Liu, J.; Wang, Z.; Hu, W. 25th Anniversary Article: Key Points for High-Mobility Organic Field-Effect Transistors. *Adv. Mater.* **2013**, *25*, 6158–6183.
- (62) Sirringhaus, H.; Brown, P. J.; Friend, R. H.; Nielsen, M. M.; Bechgaard, K.; Langeveld-Voss, B.; Spiering, A.; Janssen, R.; Meijer, E. W.; Herwig, P.; de Leeuw, D. M. Two-Dimensional Charge Transport in Self-Organized, High-Mobility Conjugated Polymers. *Nature* **1999**, *401*, 685–688.
- (63) Osterbacka, R.; An, C. P.; Jiang, X. M.; Vardeny, Z. V. Two-Dimensional Electronic Excitations in Self-Assembled Conjugated Polymer Nanocrystals. *Science* **2000**, *287*, 839–842.
- (64) Kim, H. J.; Lee, H. H.; Kim, J. W.; Jang, J.; Kim, J.-J. Surface Dependent Thermal Evolution of the Nanostructures in Ultra-Thin Copper(II) Phthalocyanine Films. *J. Mater. Chem.* **2012**, *22*, 8881–8886.
- (65) Korodi, I. G.; Lehmann, D.; Hietschold, M.; Zahn, D. R. T. Improving the Mobility of CuPc OFETs by Varying the Preparation Conditions. *Appl. Phys. A: Mater. Sci. Process.* **2013**, *111*, 767–773.
- (66) Yusuke, F.; Rongbin, Y.; Koji, O.; Kazume, N.; Mamoru, B. Improved Organic Thin Film Transistor Performance Utilizing a DH-a6T Submonolayer. *Mol. Cryst. Liq. Cryst.* **2013**, *580*, 110–116.
- (67) Hu, Y.; Gu, W.; Liu, N.; Zhu, Z.; Zhang, J.; Wang, J. Fabricating Organic Transistors Based on Domain-Ordered Copper Phthalocyanine Film Grown on Oligothiophene Epitaxial Substrate. *Phys. Status Solidi RRL* **2013**, *7*, 558–561.
- (68) Wang, H.; Zhou, Y.; Roy, V. A. L.; Yan, D.; Zhang, J.; Lee, C.-S. Polymorphism and Electronic Properties of Vanadyl-Phthalocyanine Films. *Org. Electron.* **2014**, *15*, 1586–1591.
- (69) Kraus, M.; Richler, S.; Opitz, A.; Brütting, W.; Haas, S.; Hasegawa, T.; Hinderhofer, A.; Schreiber, F. High-Mobility Copper-Phthalocyanine Field-Effect Transistors with Tetratetracontane Passivation Layer and Organic Metal Contacts. *J. Appl. Phys.* **2010**, *107*, 094503.
- (70) Kraus, M.; Haug, S.; Brütting, W.; Opitz, A. Achievement of Balanced Electron and Hole Mobility in Copper-Phthalocyanine Field-Effect Transistors by using a Crystalline Aliphatic Passivation Layer. *Org. Electron.* **2011**, *12*, 731–735.
- (71) Fai Lo, M.; Wang, H.; Liu, Z.; Wai Ng, T.; Lee, C.-S.; Yan, D. Electron Depletion and Accumulation Regions in n-Type Copper-Hexadecafluoro-Phthalocyanine and Their Effects on Electronic Properties. *Appl. Phys. Lett.* **2012**, *100*, 103302.
- (72) Ye, R.; Ohta, K.; Baba, M. *In-Situ* Study of pn-Heterojunction Interface States in Organic Thin Film Transistors. *Thin Solid Films* **2014**, *554*, 137–140.
- (73) Sinha, S.; Wang, C.-H.; Mukherjee, M.; Yang, Y.-W. The Effect of Gate Dielectric Modification and Film Deposition Temperature on the Field Effect Mobility of Copper(II) Phthalocyanine Thin-Film Transistors. *J. Phys. D Appl. Phys.* **2014**, *47*, 245103.
- (74) Liu, Q.; Li, Y.; Wang, X.; Huang, W.; Ma, J.; Li, Y.; Shi, Y.; Wang, X.; Hu, Z. Enhancing Charge Transport in Copper Phthalocyanine thin Film by Elevating Pressure of Deposition Chamber. *Org. Electron.* **2014**, *15*, 1799–1804.
- (75) Rajesh, K. R.; Kannan, V.; Kim, M. R.; Chae, Y. S.; Rhee, J. K. High Mobility Polymer Gated Organic Field Effect Transistor Using Zinc Phthalocyanine. *Bull. Mater. Sci.* **2014**, *37*, 95–99.
- (76) Babajanyan, A.; Enkhtur, L.; Khishigbadrakh, B.-E.; Melikyan, H.; Yoon, Y.; Kim, T.; Kim, S.; Lee, H.; Lee, K.; Friedman, B. Anisotropic Electric Properties of Copper(II)-Phthalocyanine Thin Films Characterized by a Near-Field Microwave Microscope. *Curr. Appl. Phys.* **2011**, *11*, 166–170.
- (77) Yadav, S.; Sharma, A.; Ghosh, S. Organic Transistor and Inverter Based on Assembly of Organic Nanowires Achieved by Optimizing Surface Morphology. *Appl. Phys. Lett.* **2013**, *102*, 093303.
- (78) Sethuraman, K.; Kumar, P.; Santhakumar, K.; Ochiai, S.; Shin, P.-K. Fluorinated Copper-Phthalocyanine-Based n-Type Organic Field-Effect Transistors with a Polycarbonate Gate Insulator. *J. Korean Phys. Soc.* **2012**, *61*, 113–118.
- (79) Ling, M. M.; Bao, Z. Copper Hexafluorophthalocyanine Field-Effect Transistors with Enhanced Mobility by Soft Contact Lamination. *Org. Electron.* **2006**, *7*, 568–575.
- (80) Li, J.; Zhang, L.; Zhang, X.-W.; Zhang, H.; Jiang, X.-Y.; Yu, D.-b.; Zhu, W.-Q.; Zhang, Z.-L. Reduction of the Contact Resistance in Copper Phthalocyanine Thin Film Transistor with UV/Ozone treated Au Electrodes. *Curr. Appl. Phys.* **2010**, *10*, 1302–1305.

- (81) Chen, F.-C.; Kung, L.-J.; Chen, T.-H.; Lin, Y.-S. Copper Phthalocyanine Buffer Layer to Enhance the Charge Injection in Organic Thin-Film Transistors. *Appl. Phys. Lett.* **2007**, *90*, 073504.
- (82) Yadav, S.; Kumar, P.; Ghosh, S. Optimization of Surface Morphology to Reduce the Effect of Grain Boundaries and Contact Resistance in Small Molecule Based Thin Film Transistors. *Appl. Phys. Lett.* **2012**, *101*, 193307.
- (83) Krzywiecki, M.; Grządziel, L.; Bodzenta, J.; Szuber, J. Comparative Study of Surface Morphology of Copper Phthalocyanine Ultra Thin Films Deposited on Si(111) Native and RCA-Cleaned Substrates. *Thin Solid Films* **2012**, *520*, 3965–3970.
- (84) Robertson, J. High Dielectric Constant Oxides. *Eur. Phys. J. Appl. Phys.* **2004**, *28*, 265–291.
- (85) Roth, F.; Huth, M. High- κ Field-Effect Transistor with Copper-Phthalocyanine. *J. Phys. D: Appl. Phys.* **2011**, *44*, 375102.
- (86) Tang, W. M.; Aboudi, U.; Provine, J.; Howe, R. T.; Wong, H.-S. P. Improved Performance of Bottom-Contact Organic Thin-Film Transistor Using Al Doped HfO₂ Gate Dielectric. *IEEE Trans. Electron Devices* **2014**, *61*, 2398–2403.
- (87) Wang, L.; Li, Y.; Song, X.; Liu, X.; Zhang, L.; Yan, D. Improved Interfacial and Electrical Properties of Vanadyl-Phthalocyanine Metal-Insulator-Semiconductor Devices with Silicon Nitride as Gate Insulator. *Appl. Phys. Lett.* **2013**, *103*, 243302–243304.
- (88) Wang, L.; Qin, H.; Zhang, W.; Zhang, L.; Yan, D. High Reliability of Vanadyl-Phthalocyanine Thin-Film Transistors Using Silicon Nitride Gate Insulator. *Thin Solid Films* **2013**, *545*, 514–516.
- (89) Morse, G. E.; Bender, T. P. Boronsubphthalocyanines as Organic Electronic Materials. *ACS Appl. Mater. Interfaces* **2012**, *4*, 5055–5068.
- (90) Lozzi, L.; Santucci, S. Au/CuPc interface: A Valence Band Photoemission Investigation. *J. Chem. Phys.* **2011**, *134*, 114709.
- (91) Lindner, S.; Treske, U.; Knupfer, M. The Complex Nature of Phthalocyanine/Gold Interfaces. *Appl. Surf. Sci.* **2013**, *267*, 62–65.
- (92) Molodtsova, O. V.; Aristov, V. Y.; Zhilin, V. M.; Ossipyan, Y. A.; Vyalikh, D. V.; Doyle, B. P.; Nannarone, S.; Knupfer, M. Silver on Copper Phthalocyanine: Abrupt and Inert Interfaces. *Appl. Surf. Sci.* **2007**, *254*, 99–102.
- (93) Coppédé, N.; Ciccoira, F.; Iannotta, S.; Martel, R. Ambipolar Copper Phthalocyanine Transistors with Carbon Nanotube Array Electrodes. *Appl. Phys. Lett.* **2011**, *98*, 183303–183303–183303.
- (94) Peng, Y.; Lv, W.; Yao, B.; Xie, J.; Yang, T.; Fan, G.; Chen, D.; Gao, P.; Zhou, M.; Wang, Y. Improved Performance of Photosensitive Field-Effect Transistors Based on Palladium Phthalocyanine by Utilizing Al as Source and Drain Electrodes. *IEEE Trans. Electron Devices* **2013**, *60*, 1208–1212.
- (95) Jakabovic, J.; Weis, M.; Kovac, J.; Donoval, D.; Donoval, M.; Daricek, M.; Telek, P.; Cirak, J.; Peng, Y.; Xie, J.; Lv, W.; Yang, T.; Yao, B.; Wang, Y. Photogenerated Charge Carriers in Double-Layer Organic Field-Effect Transistor. *Synth. Met.* **2013**, *175*, 47–51.
- (96) Li, J.; Zhou, F.; Lin, H.-P.; Zhu, W.-Q.; Zhang, J.-H.; Zhang, Z.-L.; Jiang, X.-Y. Enhanced Photosensitivity of InGaZnO-TFT with a CuPc Light Absorption Layer. *Superlattices Microstruct.* **2012**, *51*, 538–543.
- (97) Zhang, H.; Wang, D.; Jia, P. The Fabrication and Optical Detection of a Vertical Structure Organic Thin Film Transistor. *Opto-Electron. Rev.* **2014**, *22*, 41–44.
- (98) Huang, W.; Sinha, J.; Yeh, M. L.; Hardigree, J. F. M.; LeCover, R.; Besar, K.; Rule, A. M.; Breyse, P. N.; Katz, H. E. Diverse Organic Field-Effect Transistor Sensor Responses from Two Functionalized Naphthalenetetracarboxylic Diimides and Copper Phthalocyanine Semiconductors Distinguishable Over a Wide Analyte Range. *Adv. Funct. Mater.* **2013**, *23*, 4094–4104.
- (99) Li, X.; Jiang, Y.; Xie, G.; Tai, H.; Sun, P.; Zhang, B. Copper Phthalocyanine Thin Film Transistors for Hydrogen Sulfide Detection. *Sens. Actuators, B* **2013**, *176*, 1191–1196.
- (100) Raval, H. N.; Sutar, D. S.; Rao, V. R. Copper(II) Phthalocyanine Based Organic Electronic Devices for Ionizing Radiation Dosimetry Applications. *Org. Electron.* **2013**, *14*, 1281–1290.
- (101) Wood, R.; Bruce, I.; Moon, C. B.; Kim, W. Y.; Mascher, P. Modeling of Spiking Analog Neural Circuits Using Organic Semiconductor Thin Film Transistors with Silicon Oxide Nitride Semiconductor Gates. *Org. Electron.* **2012**, *13*, 3254–3258.
- (102) Kim, I.; Haverinen, H. M.; Li, J.; Jabbour, G. E. Enhanced Power Conversion Efficiency of *p-i-n* Type Organic Solar Cells by Employing a *p*-Layer of Palladium Phthalocyanine. *Appl. Phys. Lett.* **2010**, *97*, 203301.
- (103) Kim, I.; Haverinen, H. M.; Wang, Z.; Madakuni, S.; Kim, Y.; Li, J.; Jabbour, G. E. Efficient Organic Solar Cells Based on Planar Metallophthalocyanines. *Chem. Mater.* **2009**, *21*, 4256–4260.
- (104) Peng, Y.; Gao, P.; Lv, W.; Yao, B.; Fan, G.; Chen, D.; Xie, J.; Zhou, M.; Li, Y.; Wang, Y. Photo-Induced Balanced Ambipolar Charge Transport in Organic Field-Effect Transistors. *IEEE Photonics Technol. Lett.* **2013**, *25*, 2149–2152.
- (105) Lin, P.; Yan, F. Organic Thin-Film Transistors for Chemical and Biological Sensing. *Adv. Mater.* **2012**, *24*, 34–51.
- (106) Jaseentha, O. P.; Menon, C. S. Characterization of Optical, Electrical and Structural Properties of Silverphthalocyanine Thin Films. *J. Mater. Sci.: Mater. Electron.* **2008**, *19*, 602–606.
- (107) Miyake, Y.; Shiraiwa, Y.; Okada, K.; Monobe, H.; Hori, T.; Yamasaki, N.; Yoshida, H.; Cook, M. J.; Fujii, A.; Ozaki, M.; Shimizu, Y. High Carrier Mobility up to 1.4 cm² V⁻¹ s⁻¹ in Non-Peripheral Octahexyl Phthalocyanine. *Appl. Phys. Express* **2011**, *4*, 021604.
- (108) Zhang, Y.; Ma, P.; Zhu, P.; Zhang, X.; Gao, Y.; Qi, D.; Bian, Y.; Kobayashi, N.; Jiang, J. 2,3,9,10,16,17,23,24-Octakis(hexylsulfonyl)-phthalocyanines with Good *n*-Type Semiconducting Properties. Synthesis, Spectroscopic, and Electrochemical Characteristics. *J. Mater. Chem.* **2011**, *21*, 6515–6524.
- (109) Williams, G.; Suttly, S.; Klenkler, R.; Aziz, H. Renewed Interest in Metal Phthalocyanine Donors for Small Molecule Organic Solar Cells. *Sol. Energy Mater. Sol. Cells* **2014**, *124*, 217–226.
- (110) Lessard, B. H.; White, R. T.; Al-Amar, M.; Plint, T.; Castrucci, J. S.; Josey, D.; Lu, Z. H.; Bender, T. P. Assessing the Potential Roles of Silicon and Germanium Phthalocyanines in Planar Heterojunction Organic Photovoltaic Devices and How Pentafluoro Phenoxylation Can Enhance π - π Interactions and Device Performance. *ACS Appl. Mater. Interfaces* **2015**, *7*, 5076–5088 (DOI: 10.1021/am508491v).
- (111) Lessard, B. H.; Dang, J. D.; Grant, T. M.; Gao, D.; Seferos, D. S.; Bender, T. P. Bis(tri-*n*-hexylsilyl oxide) Silicon Phthalocyanine: A Unique Additive in Ternary Bulk Heterojunction Organic Photovoltaic Devices. *ACS Appl. Mater. Interfaces* **2014**, *6*, 15040–15051.
- (112) Lessard, B.; Mohammad, A.; Grant, T. M.; White, R.; Lu, Z.-H.; Bender, T. P. From Chloro to Fluoro, Expanding the Role of Aluminum Phthalocyanine in Organic Photovoltaic Devices. *J. Mater. Chem. A* **2015**, *3*, 5047–5053.
- (113) Kim, D. Y.; So, F.; Gao, Y. Aluminum Phthalocyanine Chloride/C₆₀ Organic Photovoltaic Cells with High Open-Circuit Voltages. *Sol. Energy Mater. Sol. Cells* **2009**, *93*, 1688–1691.